This is to certify that the
thesis entitled

DEVELOPMENT OF A BIOMIMETIC SENSOR THROUGH MOLECULAR IMPRINTING

presented by

Lisa Marie Kindschy

has been accepted towards fulfillment
of the requirements for the

M.S. degree in Biosystems Engineering

E Castle ulja

Major Professor's Signature

April 19, 2005

Date

MSU is an Affirmative Action/Equal Opportunity Institution

DEVELOPMENT OF A BIOMIMETIC SENSOR THROUGH MOLECULAR IMPRINTING

By

Lisa Marie Kindschy

A THESIS

Submitted to
Michigan State University
in partial fulfillment of the requirements
for the degree of

MASTER OF SCIENCE

Department of Biosystems and Agricultural Engineering

2005

ABSTRACT

DEVELOPMENT OF A BIOMIMETIC SENSOR THROUGH MOLECULAR IMPRINTING

By

Lisa Marie Kindschy

Molecular imprinting is a technique for creating synthetic receptor sites in a polymer. In this research, a molecularly imprinted polymer (MIP) biomimetic sensor was formed for theophylline using a copolymer of two monomers, methacrylic acid and ethylene glycol dimethacrylate. The presence of theophylline in the biomimetic sensor was measured using cyclic voltammetry, specifically, the corresponding peak currents on the voltammograms. The peak currents of the MIP sensor in the presence and absence of theophylline were compared to the blank sensor (non-imprinted polymer).

In the initial measurements, the peak current for the MIP sensor on indium tin oxide (ITO) increased by a factor of 5.3 upon addition of theophylline compared to the blank non-imprinted MIP. The ratio of peak currents increased by a factor of 7.5 for the MIP sensor on silicon compared to the blank. The sensitivity of the MIP on ITO was between 2 - 4 mM theophylline. The concentration of theophylline that resulted in the best signal was 3 mM. The MIP sensor showed no cross reactivity to caffeine, which has a similar chemical structure. This research will provide the foundation for future work in biomimetic sensors by developing durable sensors with longer shelf lives when exposed to rugged and harsh environments.

This thesis is dedicated to my family, Steven,

Judith, Brad, and Lori Kindschy for their love, support, and encouragement.

ACKNOWLEDGEMENTS

I would like to thank all the people who helped me through this degree. First, I would like to send my deepest thanks to my family, my mom and dad, Steve and Judy, and to my siblings, Lori and Brad, for their love and support. Brad, for your unsolicited and "expert" advice, Lori for those late night slurpee runs, mom for always listening when I needed to vent, and dad for trying solve my problems and offering your great opinions.

I would also like to thank Dr. Evangelyn Alocilja for being a great mentor, advisor, and friend, and for always offering advice and positive thinking when I needed it. Without her constant encouragement and advice, this thesis would not have been possible.

I would like to thank my labmates, Finny, Maria, Zarini, and Stephen who not only helped me in the lab, but also helped to shape the person I have become through this degree. Thanks to Stephen for being a good arguing buddy and for never making the lab a dull place; Finny for being the "handyman" of the lab and helping me with all number of problems from research questions to computer issues; Maria for giving me encouragement (and distractions) when I needed it; and Zarini for giving me useful advice and helping me through the last two grueling weeks. The conversations I have had about biosensors and life will stay with me forever. Without all of you, this degree would not have been accomplished!

TABLE OF CONTENTS

LIST OF TABLES

LIST OF FIGURES

LIST OF ABBREVIATIONS

2, 4-D	2,4-Dichlorophenoxyacetic acid
3-MPS	3-(Trimethoxysilyl)propyl methacrylate
A	Ampere
AFM	Atomic force microscopy
AIBN	2,2'-Azobisisobutyronitrile
B-ITO	Blank sensor on indium tin oxide
B-Si	Blank sensor on silicon
Caf	Caffeine
DMF	N,N-Dimethylformamide
DMSO	Dimethyl Sulfoxide
EDGMA	Ethylene glycol dimethacrylate
E	Potential
E_{app}	Applied potential
E_{final}	Final potential
E_{inital}	Initial potential
E_{pa}	Peak anodic potential
E_{pc}	Peak cathodic potential
h	hour(s)
HPLC	High performance liquid chromatography
I	current

i_{pa}	Peak anodic current
i_{pc}	Peak cathodic current
ITO	Indium tin oxide
MAA	Methacrylic acid
min	minute(s)
MIP	Molecularly imprinted polymer
MIP-ITO	Molecularly imprinted polymer sensor on indium tin oxide
MIP-Si	Molecularly imprinted polymer sensor on silicon
s	second(s)
S	Siemens
Si	Silicon
Thy	Theophylline
V	Volts

CHAPTER 1: INTRODUCTION

1.1 Significance

Novel sensors are needed for the detection and quantification of toxins and other harmful molecules. A unique group of sensors uses the principle of biomimetics, where natural processes and components are imitated through artificial replicas. Molecularly imprinted polymers (MIPs) use the technique of biomimetics to create artificial receptor sites using specific monomers, the building blocks of polymers, to create tailored recognition sites for the target molecule. Biomimetic sensors using MIPs offer some interesting advantages to typical biological-based sensors, such as those using antibodies or enzymes. MIPs have a long shelf life due to the inherent strength of the polymer and are resistant to extreme conditions, such as acidic, basic, high temperature, and low moisture environments.

Molecular imprinting is the process of forming artificial receptors for a molecule that is also used as the template. The building blocks (monomers) are polymerized around the template that is used as a mold. Once polymerization is complete, the template is removed from the polymer, leaving holes that exactly match the size and shape of the original template. The polymer is now considered imprinted because holes have been created that are specific in shape and size to the template, and to which only it can rebind. This thesis will explore the use of molecularly imprinted polymers for the detection of small molecules using a biomimetic sensor.

1.2 Hypothesis

This research will demonstrate that a biomimetic sensor can be developed through the molecular imprinting technique. To demonstrate proof of concept, the target molecule in this research is theophylline. To test the hypothesis, the objectives of this research are to: (1) confirm the imprinting of the polymer; (2) attach the imprinted polymer to an indium tin oxide (ITO) electrode; (3) test the sensitivity and selectivity of the biomimetic sensor; and (4) initially test the formation of the MIP on a silicon electrode.

1.3 Specific Activities

1.3.1 Confirmation of Imprinted Polymer

The first objective of this research is to verify that a molecularly imprinted polymer can be successfully formed. This is accomplished through the comparison of light absorption measurements of the imprinted polymer and non-imprinted (blank) polymer.

1.3.2 Attachment to Electrode for Formation of Biomimetic Sensor

After successful formation of the MIP, the next goal of this research is to attach the polymer onto an electrode for use as a biomimetic sensor. The successful attachment of the MIP to the electrode is monitored using imaging by atomic force microscopy (AFM).

1.3.3 Sensitivity of the Biomimetic Sensor

The sensitivity of the MIP sensor on ITO is studied for varying concentrations of theophylline.

1.3.4. Selectivity of the Biomimetic Sensor

The selectivity of the biomimetic sensor is evaluated by testing with caffeine, a molecule that is structurally related to theophylline.

1.3.5. Biomimetic Sensor on Silicon

The final area of investigation is to initially test the biomimetic sensor on silicon.

CHAPTER 2: LITERATURE REVIEW

2.1 Molecularly Imprinted Polymers

2.1.1 Introduction

A biosensor is an analytical device that incorporates a biological recognition element (antibodies, enzymes, DNA probes, or cells) in close proximity to a transducer that converts the recognition event between the biological element and the target analyte into a quantifiable signal. A common type of biosensor is an immunosensor, which uses the binding of an antigen to an antibody to produce a measurable signal, allowing for the quantification of the antigen (Muhammad-Tahir and Alocilja, 2003; Muhammad-Tahir and Alocilja, 2004; Radke and Alocilja, 2005). In general, antigens can be in the form of microorganisms or pollutants that are capable of stimulating an immune response in the host, resulting in the production of antigen-specific antibodies. Thus, the attractiveness of the antibody-antigen biosensor is the superior specificity that results from the antigen-antibody binding such that structurally related molecules are rejected from the binding site.

Antibody-based detection is limited by the reliance on the antigen for antibody production, the expensive extraction process of the antibodies, and the highly controlled environment needed for antibody production. Consequently, research has led to the development of synthetic antibody mimics that reproduce the natural sites of antibodies. These biosensors belong to a group of devices and processes called biomimetics, which use artificial materials to mimic biological systems found in nature. These "antibody mimics" have similar and comparable performance when measured alongside their

antibody counterparts. One type of biomimetic receptor that has received considerable attention in recent years is the group called molecularly imprinted polymers (MIPs). MIPs have several attractive characteristics that make them more suitable for certain sensor applications than their immunosensor counterparts. They are very stable and robust, and are resistant to degradation or loss of sensor properties in a wide range of conditions, such as extreme temperatures, as well as acidic and basic environments (Svenson and Nicholls, 2001).

MIPs offer a viable alternative for applications where antibodies are not available or are too expensive to obtain for a particular substrate. MIPs have been successfully used for several applications, such as the stationary phase in separations using high performance liquid chromatography (HPLC) (Kempe, 1996), thin layer chromatography (Kriz et al., 1994), catalysis (Wulff, 2002), ligand-binding assays (antibody mimics) (Andersson, 1996; Surugiu et al., 2001a), and solid phase extraction (Rashid et al., 1997; Stevenson, 1999). Imprinting technology is also employed in the area of sensors and assays where MIPs are used as binding site mimics in assay systems as well as the recognition element in biosensors.

2.1.2 Molecular Imprinting Technique

The method of molecular imprinting involves the polymerization of a functional monomer and cross linker around a molecular template (process illustrated in Figure 2-1). It is important to note that while the picture is a two-dimensional representation of the process, the imprinted site that is created is three dimensional, such as that of a lock and key.

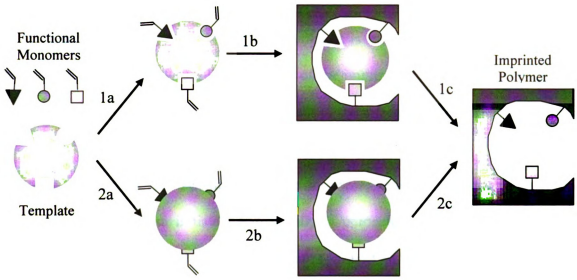

Figure 2-1. Schematic overview of molecular imprinting process. Steps of non-covalent imprinting: (1a) self-assembly, (1b) polymerization, and (1c) solvent extraction of template. Steps of covalent imprinting: (2a) synthesis of polymerizable template, (2b) polymerization, and (2c) extraction of template by chemical cleavage.

In the first step, the functional monomers are assembled around the template by either covalent or non-covalent bonds. For both methods, the process must be reversible such that the template can be removed from the polymer, but have the ability to rebind to the site. The functional monomers are selected based upon the number of bonds they can form with the template. For example, in a study on the agricultural pesticide atrazine using non-covalent interactions, the functional monomer, methacrylic acid, was chosen

for its ability to form two ionic and two-three hydrogen bonds with the template, atrazine (Sergeyeva et al., 1999). In this thesis, the term template will refer to the molecule that is used to form the molecular imprint in the polymer, and analyte will refer to the same molecule as it rebinds in the imprinted site. While these are the same compound, they differ in the purpose that each serves. The template is used as a mold around which the polymer is assembled towards the formation of the imprinted polymer. The analyte, on the other hand, is the target material that rebinds to the imprinted site that was vacated by the template and produces a measurable signal.

Following the pre-assembly step, the monomer-template complex is combined with the cross-linker, an initiator, and, usually, a porogenic solvent. The role of the porogenic solvent is to create pores or tiny holes in the finished polymer that will allow the analyte to access the imprinted binding sites. Oxygen must be removed from the reaction environment prior to polymerization either by vacuum removal or replacement with an inert gas, such as nitrogen, due to its interference with the formation of free radicals.

Polymerization is started either thermally (addition of heat) or photochemically (usually exposure to UV light) with the initiator selected based upon the requirements and restrictions of the template to either method. In a UV light initiated process, polymerization can be performed at lower temperatures. This process is preferred for non-covalent imprinting due to the increased strength of ionic and hydrogen bonding at reduced temperatures. The polymerization step fixes the position of the functional monomers around the template by creating chemical bonds between the cross linkers and

functional monomers, such that a memory of the receptor site is permanently retained in the polymer upon removal of the template.

When polymerization is complete, the template is removed by washing with an organic solvent for non-covalent imprinting or by chemical cleaving from the polymer if the covalent imprinting method is used. Subsequent processing of the polymer is usually required for bulk polymerization methods to obtain the beads that are used in many procedures (Kriz et al., 1996; Baggiani et al., 1999). After removal of the template, sites are obtained that have a chemical "memory" of the template due to the relative position of the functional monomers within the imprinted polymer.

Wulff first reported work on an organic molecularly imprinted polymer in 1973 (Wulff et al., 1973). In Wulff's research, covalent bonds were formed between the template D-glyceric acid and two other monomers (p-amino styrene and 2,3-O-p-vinylphenylboronic ester). The template-monomer complex was integrated with a divinylbenzene polymer followed by chemical cleavage of the template to obtain a binding site.

The advance in molecular imprinting technology that allowed for several new applications to emerge was the use of non-covalent bonding between the template and the functional monomers. Mosbach and co-workers found that electrostatic and hydrogen-bonding forces could be used to form a pre-assembled complex between the template phenylalanine ethyl ester and certain monomers (styrene or acrylic based) prior to polymerization, resulting in the ability to easily remove the template after polymerization with an organic solvent (Andersson et al., 1984). Non-covalent bonding has been primarily used in recent molecular imprinting procedures due to the large number of

molecules that can be imprinted using non-covalent interactions. While non-covalent imprinting is becoming mainstream, covalent imprinting may still find usefulness for certain templates or when the two techniques can be used in combination. Whitcombe combined the advantages of non-covalent and covalent bonding to produce an imprint for cholesterol (Whitcombe et al., 1995).

2.1.3 Chemical Modification of the Polymer

Polymers can be formed by a variety of different techniques with the most popular method being free radical (addition) polymerization. Other techniques include condensation polymerization, where a byproduct (usually water) is formed when the monomers combine or the use of a catalyst to facilitate the joining of monomers. MIPs are mainly formed by free radical polymerization due to the variety of functional monomers available. In this type of polymerization, the functional monomers and cross linkers generally have either a vinyl or acrylic group where monomers add onto the end of a growing chain. Prior to polymerization, a complex is formed between the functional monomers and template by the self-assembly approach. In this approach, the functional monomers bind with the template in key locations where a non-covalent bond is formed. The interactions holding the two species together in the self-assembly complex are usually based on hydrogen bonding or ionic interactions.

The selection of the functional monomers and cross-linking agent is critical to the imprinting process because the reattachment of the template to the functional monomers is the basis of the signal generation. The key element for a functional monomer is to have accessible binding sites for the interactions to occur. Several types of functional monomers and cross-linkers are available, the most common being methacrylic acid

(MAA) and ethylene glycol dimethacrylate (EGDMA). The structures of twenty common functional monomers and cross-linkers are shown in Figure 2-2.

In addition to the importance of selecting the functional monomer and cross-linker, the relative amounts of the pre-polymerization ingredients are also vital to the formation of the polymer. Various concentrations of functional monomers and cross-linkers can result in MIPs with noticeably different sensor properties. In a study by Dickert and Hayden (1999), the effect of varying the concentration of a cross-linker for both ethanol and ethanol acetate imprinting resulted in a 10% optimal cross-linker amount with the highest sensitivities and selectivities. Increasing or decreasing the amount of cross-linker in the MIP produced less accessible binding sites or decreased the imprinted effects in the sensor.

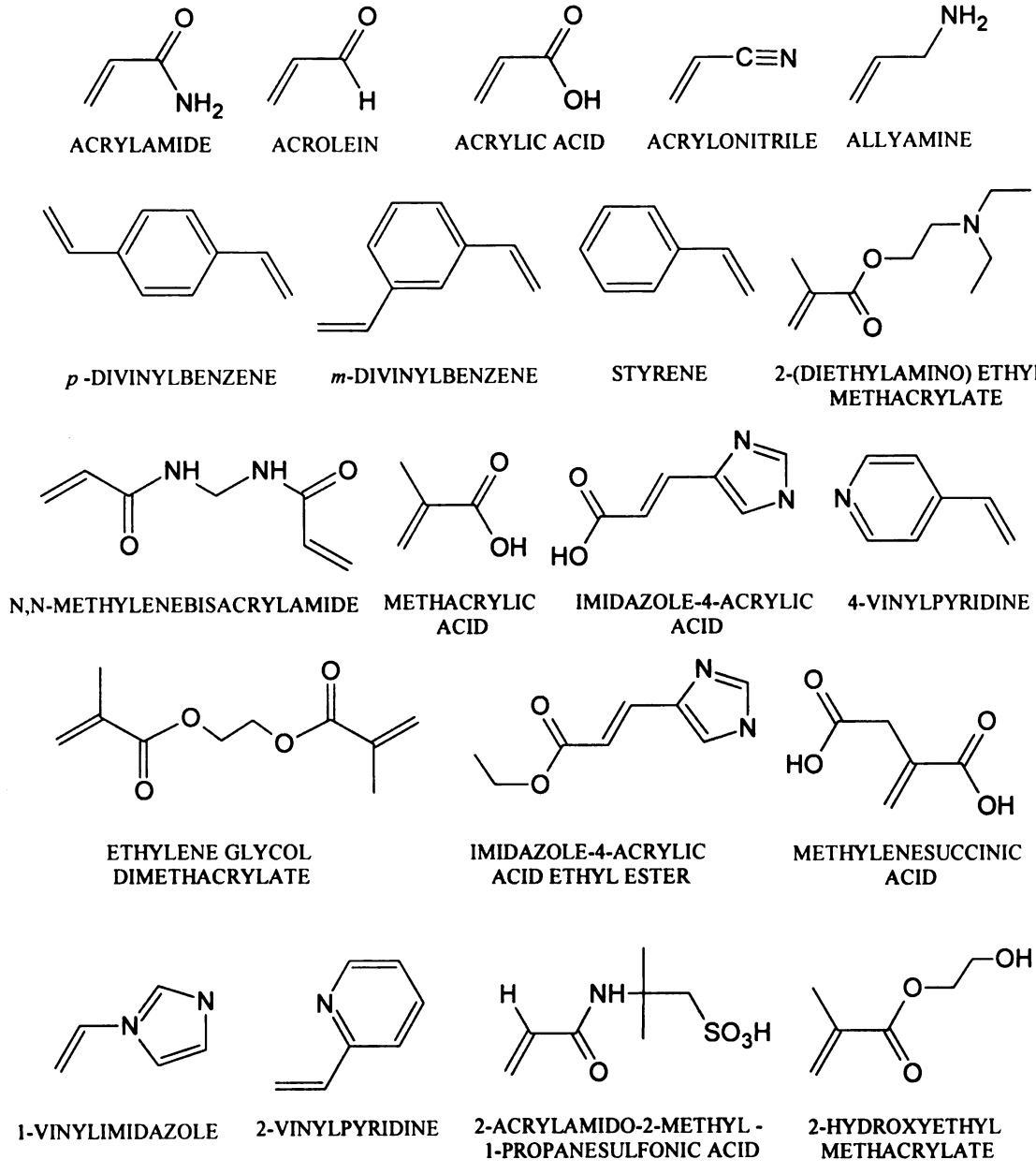

Figure 2-2. Commonly used functional monomers and cross-linkers. (Subrahmanyam et al., 2001)

2.1.4 Methods for Pre-Screening Polymers

The large number of functional monomers and cross-linkers often makes the selection process a difficult step. Assessing different functional monomers and cross-linker systems as well as various concentrations of each can be time consuming due to the tedious processing and evaluation of the resultant MIP. One technique that is used to ensure the success of an imprinted polymer involves scaling down the MIP synthesis, processing, and rebinding steps in an automated *in situ* batch process using programmed liquid-handling equipment. In a study by Takeuchi et al. (1999), the polymerization solution was dispensed into glass vials at varying monomer concentrations. They were then sealed, allowed to polymerize by UV light, and washed by repeated steps of dispensing and removing the solvent, all occurring in an automated process. A computational approach was demonstrated for microcystin-LR in which the template and a computationally designed MIP were evaluated according to their affinity, specificity, cross-reactivity, and stability and were compared to monoclonal and polyclonal antibodies (Chianella et al., 2002). An alternative method using computationally designed polymers entailed the screening of a virtual library of functional monomers against the template of interest. The functional monomer that was able to form the strongest complex with the template was selected, and real polymerization conditions were compiled using commercially available software to test the polymer (Subrahmanyam et al., 2001).

2.1.5 Physical Modification of the Polymer

Several procedures exist for modifying the physical characteristics of the polymer so that it will suit the intended application. Imprinted polymers that result from bulk polymerization in block form are relatively simple to develop, but require tedious processing to obtain the small fragments. The processing of the monolithic solid includes mechanical grinding and sieving steps to obtain small particles, and the process is inherently wasteful of chemicals (this process is commonly reported in the literature) (Kroger et al., 1999; Tan et al., 2001; Lu et al., 2002). A slightly more complicated method, typically used in chromatography, allows polymerization to occur with beads where the imprinted polymer may fill in the pores or simply coat the surface of the bead (Tamayo et al., ; Fairhurst et al., 2004). This type of polymerization allows for significantly better particle shape compared to grinding of a solid block, yet it also requires careful preparation and carries the additional cost of the original beads.

More sophisticated and complex polymerization techniques involve either a suspension in water or perfluorocarbon to produce spherical beads. The disadvantage of using a water suspension is the incompatibility with most imprinting procedures due to the disruption of interactions from the polar nature of water. The use of perfluorocarbon overcomes the interference with imprinting; however, the cost of liquid perfluorocarbon and the small literature base limit the use of this method. These suspension methods for producing imprinted polymer beads are mainly used in packed columns for chromatography. For a more detailed description of polymerization methods, refer to the article by Mayes and Mosbach (1997) and the references cited within the article.

2.1.6 Membrane Imprinted Polymers

The other polymer form that is most suited to sensor applications is a thin membrane. Thin films are ideal for sensor applications due to their uniform macroscopic shape and the variety of reproducible conditions that can be controlled during polymerization, such as the temperature, polymerization rate, and light flux (for photoinitiated polymerization). However, the inherent cross-linking nature of MIPs makes them very stiff and rigid, a property not suitable for films. Polymer films can be made more flexible and mechanically stable by the addition of a plasticizer. In the preparation of an imprinted film for atrazine, a common agricultural pesticide, oligourethane acrylate was added to the polymerization mixture containing the functional monomer methacrylic acid and triethylene glycol dimethacrylate as the cross-linker (Sergeyeva et al., 1999). Oligourethane acrylate served as the plasticizer in this procedure, making the imprinted film more flexible. The optimal ratio of cross-linker to plasticizer was found to be 85:15 (w/w) with the specificity and flexibility of the imprinted membrane maintained. To form the membrane, the polymerization mixture was placed between two quartz glass slides where polymerization occurred by the addition of UV light. The membrane thickness was between 60 and 120 μm and was used in a conductometric sensor system (Sergeyeva et al., 1999).

The use of MIPs as the recognition element in a biosensor requires the immobilization of the polymer onto the surface of the transducer. *In situ* polymerization allows the polymer to be electrically synthesized on the surface of the transducer with no after-processing requirement, excluding solvent washing for removal of the template. The film is grown onto conducting electrodes of virtually any size and shape with the

thickness controlled by the amount of charge flowing through the electrode. The first successful application of electropolymerization detected a glucose template in a poly(o-phenylenediamine) polymer matrix using a quartz crystal microbalance biomimetic sensor (Malitesta et al., 1999).

Another method for applying polymers to transducers is using a surface coating method, either spin or spray coating. In one experiment, the pre-polymerization liquid containing the imprint molecule, the functional monomer MAA, cross-linker EGDMA, photoinitiator, and solvent (toluene) were mixed and sprayed onto a gold electrode where polymerization was initiated by exposure to UV radiation (Jakoby et al., 1999). Polymer beads of uniform size can also be used in sensors by immobilization onto an electrode either in a gel or in a membrane. An imprinted polymer, poly(EGDMA-co-4-vinylpyridine), specific for the agricultural herbicide 2,4-Dichlorophenoxyacetic acid (2,4-D) was prepared by the bulk polymerization method and mechanically ground into small particles that were suspended in acetone. The particles that remained in suspension after 4 h of settling time were collected. The collected particles were resuspended in methanol, pipetted onto a screen-printed electrode, and allowed to dry. The particle layer was covered with a hot agarose solution to form a permeable membrane over the electrode (Kroger et al., 1999).

Thin polymer layers can also be formed by adhesion to other surfaces. For the preparation of a thin membrane for sensing of theophylline, an indium-tin oxide film was washed and placed in a solution of MAA, EGDMA, template, and a photoinitiator, allowed to polymerize, and ultrasonicated to remove weakly adhering copolymer (Yoshimi et al., 2001). Another procedure developed a flow injection capillary imprinted

with 2,4-D in the presence of 4-vinylpyridine (functional monomer) and trimethylolpropane trimethacrylate (cross-linker). The activated capillaries were filled with the functional monomer and cross-linker solutions with an initiator where polymerization was carried out in a water bath. To remove loosely adhering polymer, this procedure utilized a sonication bath after rinsing with methanol to obtain a uniform polymer layer (Surugiu et al., 2001b). Similar to the capillary tube, imprinted polymer films can be polymerized between two glass slides (Duffy et al., 2002). For a more extensive review of emerging MIP formats, refer to the article by Pérez-Moral and Mayes (2002).

2.1.7 Transducer Selection

In addition to the recognition element, the other component of a biosensor is the transducer, which converts the recognition event into a measurable electric signal. The binding of the analyte to the antigen can be verified by optical, piezoelectric, or electrochemical devices. The two most common methods are electrochemical and optical due to ease of measuring and the availability of instrumentation. The selection of the transducer depends on many factors, such as the nature of the analyte, temperature range, presence of corrosive materials, atmospheric/gaseous conditions, size or weight constraints, and desired sensitivity (Haupt and Mosbach, 2000; Merkoçi and Alegret, 2002).

Electrochemical sensor devices can be subdivided into four categories: amperometry, potentiometry, conductometry, and impedance measuring sensors. Amperometric sensors measure the current at a fixed voltage and are widely used due to their simplicity and low cost. Potentiometric sensors measure the voltage at zero or near

zero current. The potential is measured between a working electrode and a reference electrode. Measurements using both amperometry and potentiometry are made either in steady-state or transient conditions since an equilibrium response is not possible. Conductive sensors measure the change in conductivity over time as a result of the analyte binding to the receptor. Impedance devices measure the total electrical resistance when an alternating current is passed through a specific medium, such as a polymer membrane (Blanco-Lopez et al., 2004).

Other transduction formats include piezoelectric, which measures changes in mass, and optical, which monitors the emission or adsorption of electromagnetic radiation such as spectrometry, fluorimetry, surface plasmon resonance (SPR), and luminescence (Yano and Karube, 1999). Table 2-1 summarizes different methods of detection in sensors and the monomer-analyte system used in each study.

Table 2-1. Summary of Molecularly Imprinted Polymers in Sensor Applications (Reproduced from Yano and Karube, 1999).

Class	Analyte	Functional Monomer	Detection Range	Reference
Spectrometry	Chloramphenicol	DEAEM	1 to 1000 μg/mL	Levi et al., 1997
	Chloramphenicol	DEAEM	3 to 30 μg/mL	McNiven et al., 1998
	Testosterone	MAA	0.10 to 1.25 mM	Cheong et al., 1998
Fluorimetry	Triazine	MAA	0.01 to 100 mM	Piletsky et al., 1997
	Sialic acid	Allylamine + TVPhB	0.5 to 10 μM	Piletsky et al., 1996
	Dansyl-L-pheneylalanine	MAA, 2Vpy	0 to 30 μg/mL	Kriz et al., 1995b
	Pyrene	Aromatic polyurethane	0 to 40 μg/L	Dickert et al., 1998a
	cAMP	DMASVBP + HEMA	0.1 to 100 μM	Turkewitsch et al., 1998
	NATA	HEAPTES + TES	Qualitative	Lulka et al., 1997
Conductometry	Atrazine	DEAEM	0.01 to 0.5 mg/L	Piletsky et al., 1995
	Sialic acid	Allylamine + TVPhB	1 to 50 μM	Piletsky et al., 1998
	Morphine	MAA	Qualitative	Kriz et al., 1995a
	L-Phenylalanine	DEAEM	0.05 to 0.4 mM	Piletsky et al., 1994
pH	Glucose	STACNCu	0 to 25 mM	Chen et al., 1997
Capacitance	Phenylalanine anilide	MAA	Qualitative	Hedborg et al., 1993
Amperometry	Morphine	MAA	0.1 to 10 μg/mL	Kriz and Mosbach, 1995
Luminescence	PMP	DVMB	0.125 to 150,000 μg/L	Jenkins et al., 1997
Potentiometry	Phenylalanine anilide	MAA	33 to 3300 μg/mL	Andersson et al., 1990
SAW, QMB	*o*-Xylene	Aromatic polyurethane	Qualitative	Dickert et al., 1998b
SPR	Theophylline	MAA	0.4 to 6 mg/mL	Lai et al., 1998

Abbreviations:

cAMP = adenosine 3P:5P-cyclic monophosphate
DEAEM = diethylaminoethyl methacrylate
DMASVBP = trans-4-[p-(N,N-dimethylamino) styryl]-N-vinylbenzylpyridinium chloride
DVMB = 3,5-methyl divinyl benzoate
HEAPTES = bis(2-hydroxyethyl)-aminopropyltriethoxysilane
HEMA = 2-hydroxyethyl methacrylate
MAA = methacrylic acid
NATA = N-acetyltryptophanamide
PMP = pinacolyl methyl phosphonate
QMB = quartz microbalance
SAW = surface acoustic wave
SPR = surface plasmon resonance
STACNCu = Cu[1-(4P-vinylbenzyl)-1,4,7-triazacyclononane]SO_4
TES = tetraethoxysilane
TVPhB = tris(4-vinylphenyl)boroxine
2Vpy = 2-vinylpyridine

2.1.8 Food and Agricultural Applications of MIPs

2.1.8.1 Food Applications

In recent years, people have become more health conscious, leading to adjustments in food preparation and handling. Changes in lifestyle and attitude have led to the consumption of raw and fresh foods that are minimally processed, with importance given to those that are low in fat, sugar, and preservatives. These shifts in food preparation and handling create a more suitable environment for the growth of microorganisms. The result is an increased need for fast, cost-effective biosensors with a high degree of sensitivity and selectivity for the detection of pathogens, microorganisms, toxins, and pesticides in food and water. This demand has sparked the need for sensors to rapidly identify any adulteration that may be present in food or water. By the year 2005, the food pathogen testing market is anticipated to grow to $192 million per year with 34 million tests to be performed (Alocilja and Radke, 2003). The first study to report a MIP-like technique for pathogen detection used a surface imprinting technique for *Listeria monocytogenes* and *Staphylococcus aureus* to synthesize a polyamide layer around the template bacteria, forming a microcapsule (Aherne et al., 1996). While this is not produced like conventional imprinted polymers, the research leading in this direction will be critical to detecting microbial food and water contaminants with MIP sensors.

The most widely imprinted templates for food applications are small molecules, such as sugars, peptides, proteins, vitamins, oils, colorants, preservatives, and toxins. In a study by Lai et al. (1998), MIPs were produced for three drugs, including caffeine, using a surface plasmon biosensor. In a later study, a bulk acoustic wave (BAW) sensor for caffeine was developed using a spin coating method of ground MIP particles (Liang et

al., 1999). The detection limit of the sensor was 5.0×10^{-9} M, with a response range between 5.0×10^{-9} M and 1.0×10^{-4} M. Several other food components have been successfully incorporated into MIP sensors, such as cholesterol (Piletsky et al., 1999), flavonol (Suarez-Rodriguez and Diaz-Garcia, 2000), and methyl-β-glucose (Chen et al., 1997). The variety of small compounds that can potentially be imprinted allows the development of sensors to detect possible harmful substances in food such as toxins and allergens. A recent review discussing MIPs for food monitoring applications including sensors, liquid chromatography, and solid phase extraction is available (Ramström et al., 2001).

2.1.8.2 Agricultural Applications – Pesticides, Toxins, and Biowarfare Agents

In the agricultural sector, the detection of pesticides that control unwanted plants, insects, fungi, and microorganisms requires novel approaches to monitor the levels specified by governmental agencies. MIPs constitute an emerging technology in agricultural sensing that overcomes some drawbacks of other methods, such as the reliance on antibodies and the irreversible binding that inhibits reuse of some sensors. Several studies have been conducted on agricultural contaminants, many in the sensing area. As previously described, a competitive electrochemical sensor for the herbicide 2,4-D was developed by immobilizing imprinted particles with an average diameter of 1 μm onto screen-printed electrodes. The sensor response was measured using differential pulse voltammetry, with the time for one scan taking 15 s (30 min to 1 h to reach equilibrium) (Kroger et al., 1999). Several branch studies have been performed using 2,4-D in other sensor formats, such as a thin MIP on the surface of a silicon wafer studied with a radio ligand binding assay (Yan and Kapua, 2001). Two similar studies employed

chemiluminescence to detect 2,4-D in a setup similar to an enzyme-linked immunosorbent assay using a MIP as the receptor instead of the antibody (Surugiu et al., 2001a; Surugiu et al., 2001b). MIPs have been formed for other herbicides, such as an imprinted polymer coating for desmetryn onto a polypropylene support film using grafting photopolymerization (Panasyuk-Delaney et al., 2001). This sensor used capacitive detection to test the response for desmetryn against triazine derivatives and found the sensor to be fairly specific to the target molecule. As mentioned in the previous discussion on thin film MIPs, a conductometric membrane sensor for atrazine was prepared from MAA and EGDMA with the addition of a plasticizer to increase the flexibility of the membrane (Sergeyeva et al., 1999). The response time of the sensor varied from 12-15 min for a 120 μm membrane to 6-10 min for a 60 μm membrane, with the imprinted membranes having excellent specificity to atrazine compared to similar herbicides.

A thin-layer MIP for the pesticide hexachlorobenzene was attached to a quartz crystal microbalance (Das et al., 2003). High selectivities compared to four structurally similar compounds and sensitivities as low as 10^{-12} mol/L were obtained for this MIP with a response time of approximately 10 s. Promising results were also obtained for an optical MIP sensor for pesticide and insecticide detection in water where the detection limit was less than 10 parts per trillion with a response time of less than 15 min (Jenkins et al., 2001). A recent study demonstrated the successful formation of a MIP for the herbicide metsulfuron-methyl (Zhu et al., 2002). These studies show that research into the fabrication of real-time, sensitive, and selective sensors for pesticide detection can be initiated since many of these MIPs have been proven successful.

Studies have also demonstrated that MIPs can be formed for toxins and biological agents. While these molecules are not used in sensors, they are worth noting for future sensor applications in agriculture and biosecurity. A potentially carcinogenic mycotoxin produced by several species of fungi, ochratoxin A, was used in MIPs for solid phase extraction (Jodlbauer et al., 2002) and liquid chromatography (Baggiani et al., 2002). Two MIPs for the mycotoxins deoxynivalenol and zearalenone were shown to be successful through HPLC analysis (Weiss et al., 2003). Future studies can strive to link the above three MIPs to a transducer for use in sensing devices.

The design of a polymer specific for microcystin-LR, a toxin produced by several species of cyanobacteria, had a detection limit of 0.1 μg/L using an enzyme-linked competitive assay (Chianella et al., 2002). A silane-imprinted polymer was successfully formed for conotoxin, a neurotoxin found in snails of the *Conus* genus (Iqbal et al., 2000). The results of the study indicated that silane-imprinted polymers could recognize subtle structural differences between two closely related conotoxins. Another silane-imprinted polymer specific for ricin, a potent toxin from castor beans and potential biowarfare agent, was confirmed by fluorescence binding detection and showed a high affinity to the imprinted sites (Lulka et al., 2000; Piletsky et al., 2001a). The detection of this large toxin exhibits potential for producing MIPs for other larger molecules and biological toxins.

2.1.9 Potential Applications

A surge in the number of groups working with MIPs (a rise from about 8 to 70 from 1990 to 1999) and the number of papers being published (a rise from about 12 to 119 from 1990 to 1999) shows that interest in imprinting technology is expanding with

continual opportunities for research (Piletsky et al., 2001a). Imprinting technology has the ability to be used in separation systems, such as water purification, wastewater treatment, and in the chemical and pharmaceutical industries. The potential market for biosensors in drug testing, drug delivery, *in vitro* diagnostics, military (warfare agent detection), and electronic noses and tongues is $1.9, $1, $19, $0.64, and $4 billion, respectively (Piletsky et al., 2001b). The use of MIPs in the solid phase extraction of drugs and in drug separation is of growing interest as well as applications for drug screening and *in vivo* monitoring. The ability of MIPs to retain receptor properties under extreme conditions without loss of recognition may be very important in aeronautical situations of low gravity and in situations of extreme pressures or temperatures due to the stability of the polymer compared to other receptors such as antibodies. MIPs will also be critical for military applications for the detection of biological warfare agents such as toxins as well as the detection of compounds used for explosives where the stability of the sensor and the long shelf life (up to six months for some MIPs) will be vital to the sensor.

2.1.10 Limitations and Challenges

The ability to incorporate MIPs with sensors combined with the stability, resistance, and shelf life of the recognition sites allows for a new array of biosensors that do not require controlled environments, as is the case for antibodies. The potential applications for MIPs in the field of biosensors and assay systems are limited by the research on MIP systems that is currently available. The number of templates that can be successfully imprinted is constantly increasing as new functional monomer-template combinations are assembled. Although a variety of imprinted polymers can be produced,

the lack of a general procedure for their preparation and confirmation of binding sites limits the surge of industrial interest in this technology. Often the presence of background noise due to the remaining template in the receptor sites can interfere with the signal, especially in fluorescence type systems. Future research will also focus on the development of MIPs for use in water and other polar-based solvent systems as well as increasing the sensitivity and selectivity of current imprinted polymer systems.

Studies recently published have shown that certain templates can be successfully imprinted, but there is a lack of feasible applications for the resulting imprinted polymers. Most imprinting technology arises from specialized groups that seek to extend and improve current methods and monomer systems. The challenge for future researchers will be to find real-world applications for current polymer systems that are rapidly being produced. The ability to link an imprinted polymer with a suitable transducer that allows for quantitative measurements of the binding of the analyte will be critical to the incorporation of MIP receptors into real-time sensors. In the near future, imprinting technology has the potential to become mainstream alongside current biosensors and to offer real alternatives in sensing systems.

2.2 Cyclic Voltammetry

Electrochemical techniques explore the interplay between electricity and chemistry. It specifically examines the role of charge, current, or potential, to changes in chemical parameters, such as the concentration of a particular compound. Potentiometric methods measure an electron transfer reaction by applying a potential and measuring the resulting current. The purpose of a potentiometric technique is to acquire a current response that is related to the concentration of the target analyte. Cyclic voltammetry is a

potentiometric method that applies a triangular potential waveform to the system under investigation resulting in a current response (Figure 2-3).

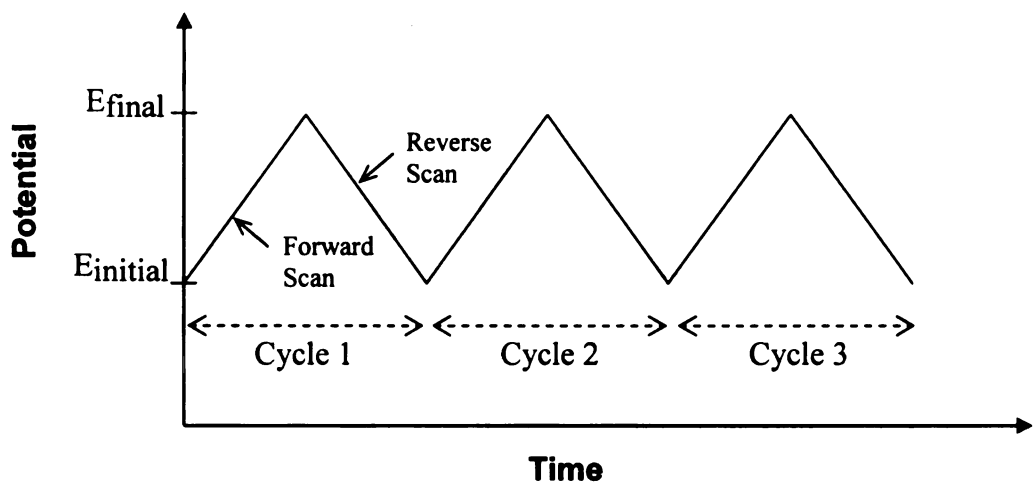

Figure 2-3. Excitation signal for a cyclic voltammetry experiment. (Adapted from Wang, 2000)

Cyclic voltammetry varies the potential to obtain information about the redox process of the system and to obtain the values of the redox potentials. A typical cyclic voltammogram for a reversible process is shown in Figure 2-4. The potential is plotted on the x-axis with the measured current values plotted on the y-axis. The values of interest on a cyclic voltammogram are the two peak currents and the corresponding potentials. The cathodic peak current, i_{pc}, and the anodic peak current, i_{pa}, occur at the reduction point and oxidation point, respectively (Bard and Faulkner, 2000).

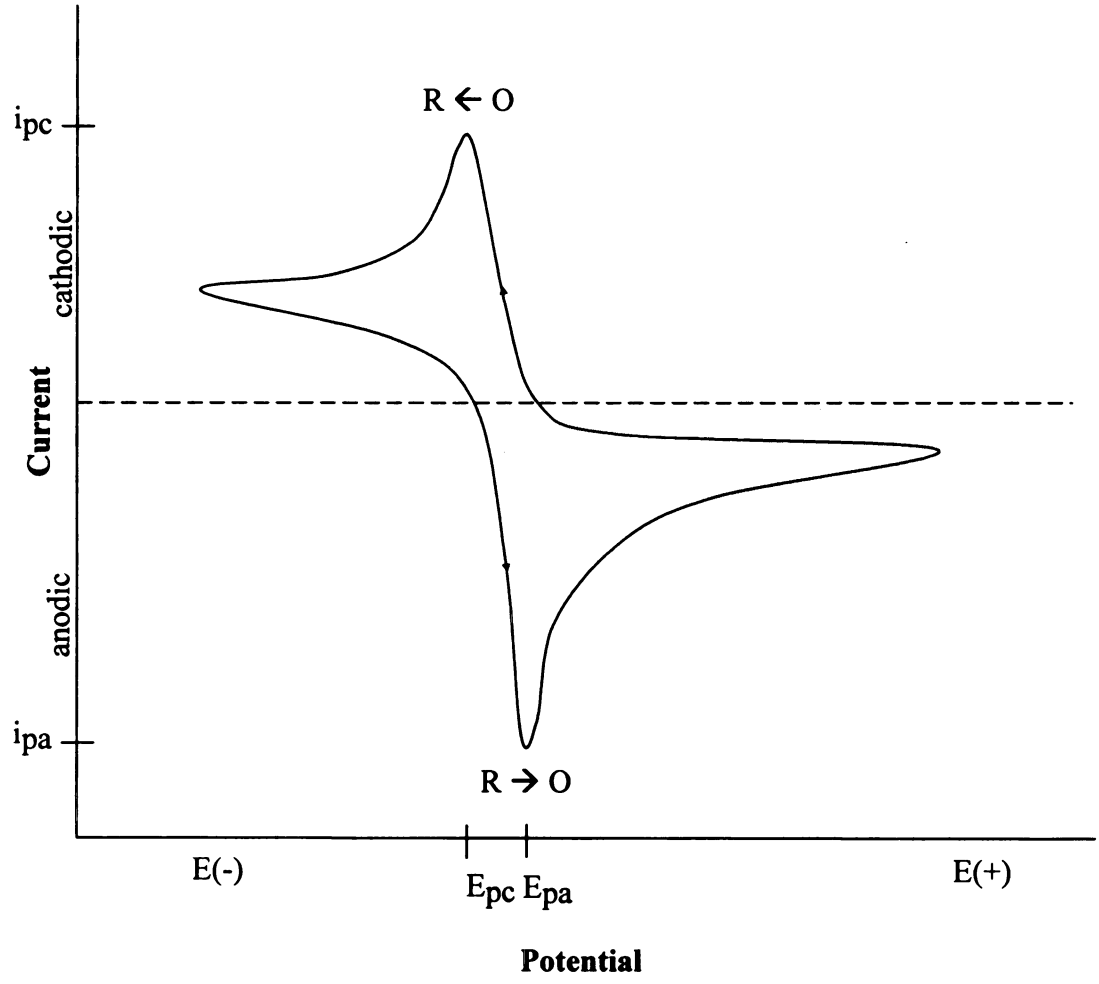

Figure 2-4. Typical cyclic voltammogram for a reversible system.

In cyclic voltammetry experiments, the current is measured in a three-electrode electrochemical cell. The electrochemical cells used in this research are further discussed in chapter 3 (Section 3.4). The schematic representation of a three-electrode potentiostat is shown in Figure 2-5. In a potentiostat, the current is supplied through the counter electrode and is measured through the working electrode. The response of the working electrode depends on the concentration and composition of the analyte being measured. The third electrode is a reference electrode that provides a constant reference potential against which the working electrode measures the output current. The reference electrode draws little or no current from the system and is unresponsive to the composition of the species under measurement (Bard and Faulkner, 2000).

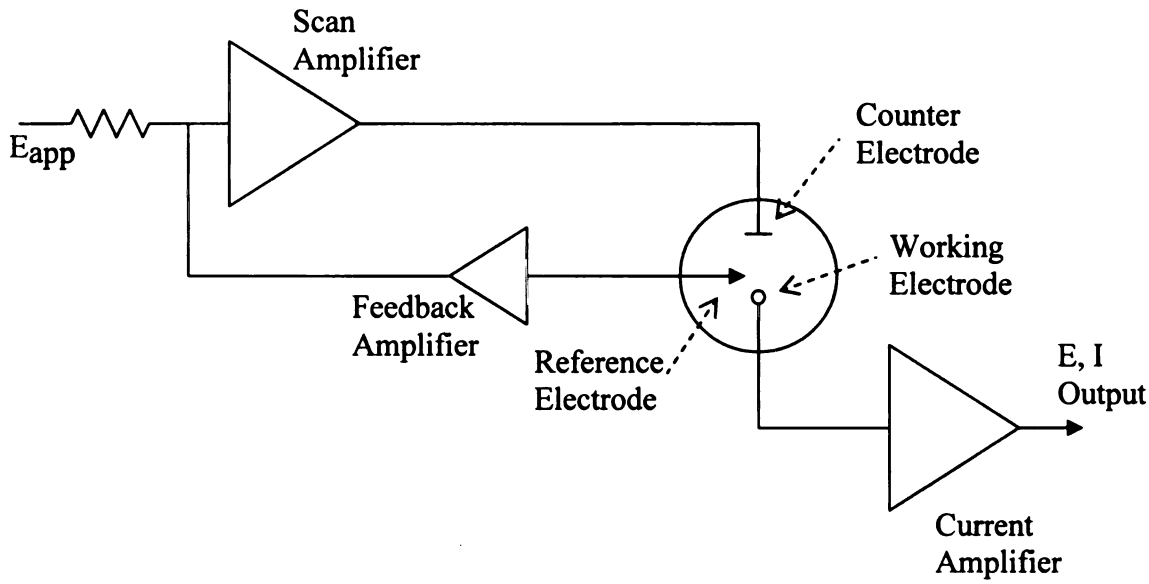

Figure 2-5. Schematic representation of a three-electrode potentiostat. (Adapted from Wang, 2000)

Cyclic voltammetry measures the faradaic current, or the current as a result of electron transfer. Two factors can affect the faradaic current: the rate at which the redox species diffuses to the electrode and the rate of electron transfer. The rate the species diffuses to the electrode surface is discussed in Section 4.1 as it applies to this research.

The rate of electron transfer for the common redox couple $Fe(CN)_6^{3-/4-}$ is reasonably fast. The reaction at the working electrode or cathode is

$$Fe(CN)_6^{3-} + e^- \leftrightarrow Fe(CN)_6^{4-}$$

where one electron is added to the ferricyanide anion to reduce iron from the +3 to the +2 oxidation state. This reaction proceeds in both directions so that species can be oxidized to $Fe(CN)_6^{3-}$, then reduced back to $Fe(CN)_6^{4-}$ (Pine Instrument Company).

CHAPTER 3: METHODS AND MATERIALS

3.1 Overview of Procedure for Research

The basic procedure for molecular imprinting with theophylline follows that of Yoshimi et al. (2001) except for the modification of the template removal procedure. Table 3-1 identifies the parts unique to this research.

Table 3-1. Procedures Used in This Research.

Procedure in This Research	**Reference**
Cleaning of ITO electrode	Yoshimi et al. 2001
Formation of MIP	Yoshimi et al. 2001
Removal of template	Vlatakis et al., 1993; Hong et al., 1998; Mullett and Lai, 1998
Rebinding	Yoshimi et al. 2001
Measurement	Yoshimi et al. 2001
Sensitivity	Original to this research
Selectivity at various concentrations	Original to this research
MIP on silicon measured with cyclic voltammetry	Original to this research

3.2 Chemicals

Methacrylic acid (MAA), ethylene glycol dimethacrylate (EGDMA), 2,2'-azobisisobutyronitrile (AIBN), and 3-(trimethoxysilyl)propyl methacrylate (3-MPS) were purchased from Sigma (St. Louis, MO). P-type silicon wafers (oxide layer 1 μm, conductivity 1667 S/cm) were obtained from the microfabrication laboratory at Michigan State University. Indium tin oxide (ITO) coated glass slides were acquired from Sigma (ITO coating 300-600 Å; resistance 30-60 Ω). All other chemicals were of ACS grade and used as received.

3.3 Preparation of electrodes

3.3.1 ITO electrode

The ITO coated glass slides were cut with a steel wheel glasscutter into 1.3 cm squares. Each electrode was rinsed twice with methanol followed by rinsing twice with deionized water, and dried under nitrogen environment.

3.3.2 Silicon electrode

The silicon electrodes were cut with a diamond tipped pen into 1.3 cm squares. These electrodes were soaked in hydrofluoric acid for 5 min to remove the surface oxide. Following oxide removal, the silicon was cleaned by first immersing in a 1:1 v/v solution of methanol and hydrochloric acid for 30 min, and then thoroughly rinsing twice with deionized water. The silicon was next boiled in water for 30 min and rinsed twice with deionized water. The silicon electrodes were dried under nitrogen environment.

3.4 Electrochemical cells

Two different electrochemical cells were used for this research. Cell A, shown in Figure 3-1, was an inverted cone shape where the working electrode is placed at the bottom of the cell. The solution only contacted one side of the working electrode that was exposed through the opening on the bottom of the cell. The contact area between the electrochemical solution and the working electrode in cell A was circular with an area of 0.283 cm^2 (diameter of 0.6 cm). The reference and counter electrodes were secured at the top of the cell. The amount of liquid necessary to adequately cover the counter and reference electrodes was 25 ml for cell A.

The other electrochemical cell, cell B shown in Figure 3-2, is shaped similar to a beaker with three openings all located on the top. The reference and counter electrodes were secured at the top similar to the setup in cell A. In cell B, however, the working electrode was suspended in the electrolyte solution such that the area of the working electrode in the electrochemical solution was greater than cell A. The approximate surface area of the working electrode exposed to the solution in cell B was 1 cm^2. The height of the working electrode relative to the cell was fixed by the rubber stopper. The volume of liquid used in cell B was 50 ml to cover the three electrodes.

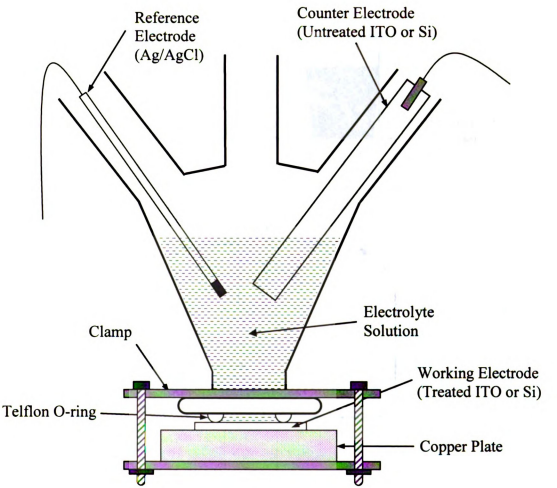

Figure 3-1. Cell A – Three-electrode electrochemical cell with working electrode at the bottom of the cell.

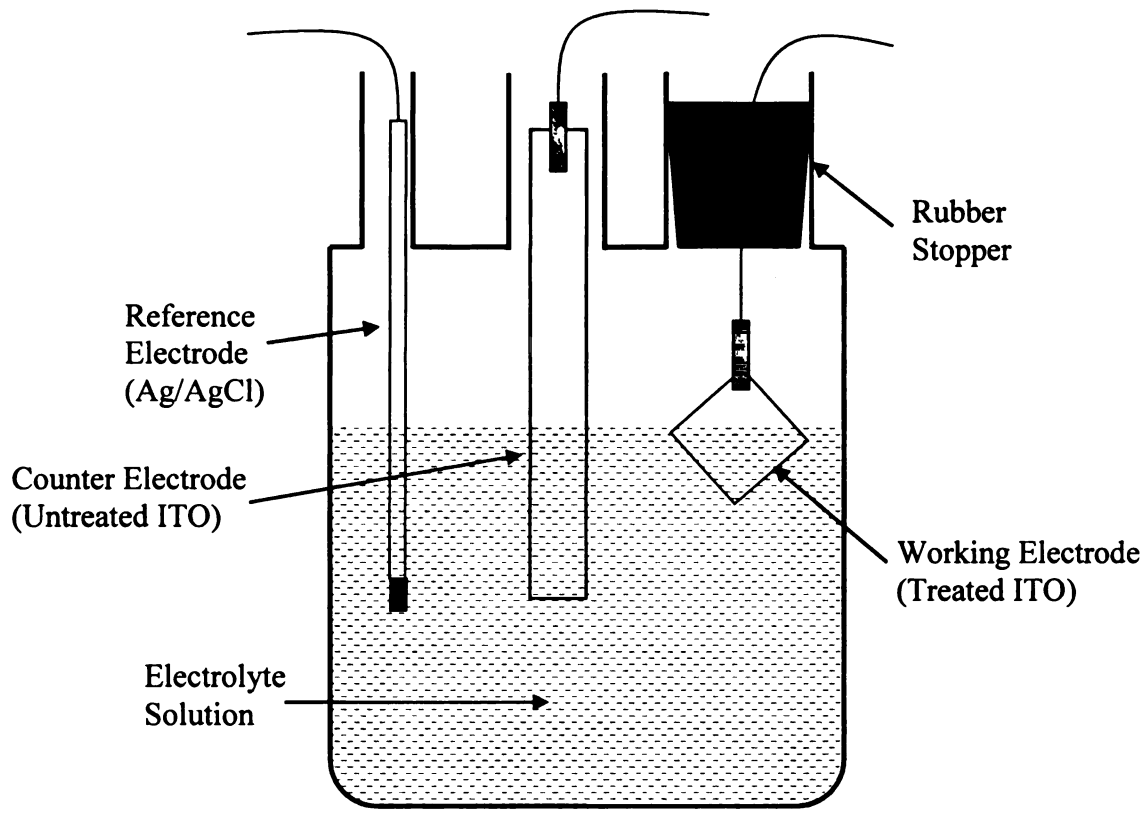

Figure 3-2. Cell B – Three-electrode electrochemical cell with working electrode submerged.

3.5 Preparation of the Theophylline Imprinted Biomimetic Sensor

The process of preparing the electrode (ITO or Si) and forming the theophylline MIP is illustrated in Figure 3-3. The formation of the MIP followed the procedure by Yoshimi et al. (2001) with some modifications. The electrode (ITO or Si) was silanized in a 10% solution (v/v) of 3-MPS in toluene for 6 h at 80°C under nitrogen atmosphere. Silanization activated the surface of the electrode, which allowed the MIP to be covalently bonded to the surface. Following silanization, the electrode was rinsed with methanol and dried under nitrogen environment. The polymer was prepared using methacrylic acid (MAA) as the functional monomer and ethylene glycol dimethacrylate (EGDMA) as the cross-linker (Figure 3-4). The initiator was 2,2'-azobisisobutyronitrile (AIBN), the porogenic solvent was *N,N*-dimethylformamide (DMF), and theophylline was used as the template. Chemical inhibitors were removed from MAA and EGDMA by passing them through an inhibitor removal column (Aldrich 30,631-2) immediately before use. MAA (0.119 ml), EGDMA (1.20 ml), AIBN (0.036 g), and theophylline (0.063 g) were added to 3.31 ml of DMF. The silanized electrode was immersed in 2 ml of the above solution and placed under nitrogen atmosphere. The electrode was allowed to polymerize for 12 h at 60°C. After this preparation, the theophylline-imprinted polymer on ITO or silicon would be referred to as the biomimetic MIP-ITO or MIP-Si sensor. A reference non-imprinted polymer (blank) to be referred to as B-ITO or B-Si, was similarly made by omitting the theophylline template.

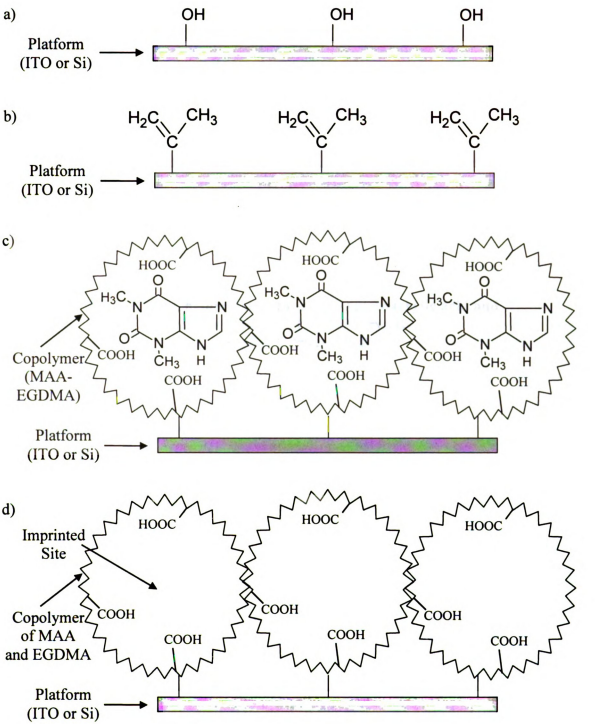

Figure 3-3. Procedure for the formation of theophylline MIP on electrode. (a) Clean electrode; (b) Silanize in 3-MPS/toluene (10% v/v) (c) Combine MAA, EDGMA, AIBN, DMF, and Thy; polymerize for 12 h at 60°C; Eliminate bulk polymer; (d) Wash with 9:1 methanol/ acetic acid for 1 h.

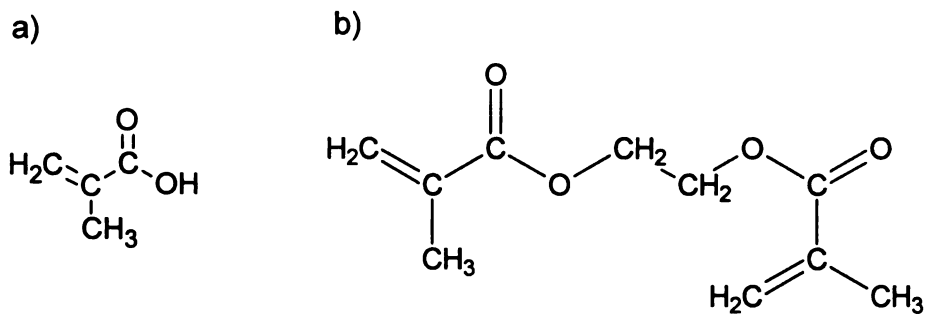

Figure 3-4. Chemical structures of (a) methacrylic acid and (b) ethylene glycol dimethacrylate. (Sigma-Aldrich, 2004)

3.6 Extraction of Template

Both the MIP and blank sensors (ITO and Si) were washed in a 9:1 v/v solution of methanol and acetic acid for 1 h. This washing removed the template and any excess polymer. The MIP and blank sensors were rinsed twice with methanol followed by rinsing twice with water and twice more with methanol. The MIP and blank sensors were stored in water until measurement to prevent drying or cracking of the polymer.

3.7 Baseline Measurement

Two electrochemical cells were used in this research. Cell A (Figure 3-1) had a circular area of the sensor exposed to the electrolyte solution with a diameter of 0.6 cm. Cell B (Figure 3-2) had both sides of the sensor exposed through a dipping format.

Before addition of the theophylline analyte, a baseline was obtained for each sensor (MIP and blank) using a blank electrolyte that was an aqueous solution of 0.1 M potassium nitrate and 5 mM potassium ferrocyanide. A volume of 25 ml (or 50 ml for cell B) was added to electrochemical cell A. Cyclic voltammetry was performed with the blank solution using a Versastat II Potentiostat/Galvanostat (Princeton Applied Research, Oak Ridge, TN). The working electrode was the treated (imprinted) material, the reference electrode was the Ag/AgCl, and the counter electrode was the untreated material (ITO or silicon). The potentiostat was run in the ramp, one vertex multi mode. The potential was cycled between –1 V to +1 V for ITO, and between –2 V to +2 V for silicon at a scan rate of 200 mV/s. The resulting current was measured and plotted against the potential. After measurement, the blank solution was discarded.

3.8 Rebinding and Measurement of Theophylline Analyte

The rebinding of the analyte was performed in the same electrochemical cell by cyclic voltammetry measurements. The analyte solution was the blank (0.1 M potassium nitrate and 5 mM potassium ferrocyanide) with the addition of the appropriate theophylline concentration. The analyte solution of 25 ml for cell A (or 50 ml for cell B) was added to the electrochemical cell and cyclic voltammetry was performed as in Section 3.7. The sensitivity of the MIP sensor was evaluated at four theophylline concentrations: 1, 2, 3, and 4 mM. Signal measurements were done according to Section 3.7.

3.9 Selectivity Evaluation

The selectivity of the MIP sensor was evaluated using caffeine, which is structurally related to the target analyte, theophylline. As shown in Figure 3-5, the structures of theophylline and caffeine differ only in the group attached to the nitrogen atom. In theophylline, this group is a single hydrogen atom while in caffeine this is a CH_3 group. This slight structural difference makes caffeine ideal for testing the crossreactivity of the theophylline-imprinted polymer sensor. The selectivity testing was performed using four concentrations of caffeine: 1, 2, 3, and 4 mM.

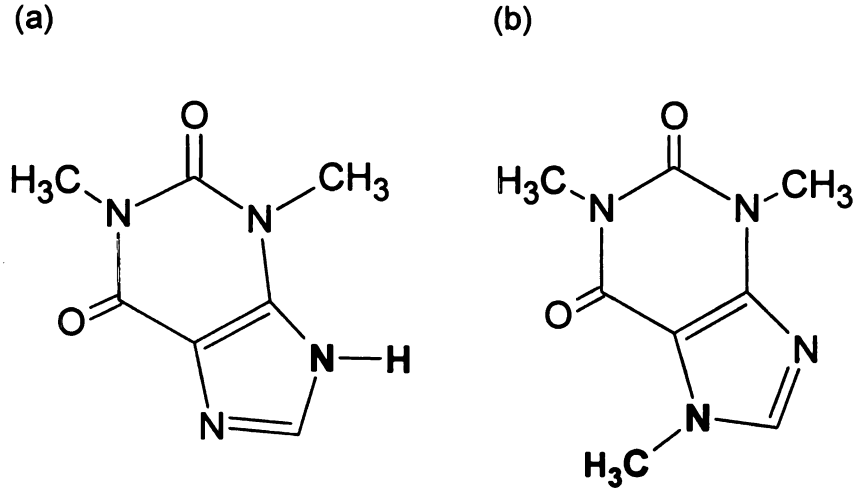

Figure 3-5. Chemical structures of (a) theophylline and (b) caffeine. (Sigma-Aldrich, 2004)

3.10 Light Absorbance Measurements

The MIP and blank polymer were prepared according to Section 3-5. Following template removal for 1 h in 9:1 methanol/acetic acid, 50 mg of both the MIP and non-imprinted polymer was removed, weighed, and rebound with the analyte separately. The rebinding concentration of 5 mM theophylline was combined with each of the polymers and allowed to soak for 25 min. After rebinding, each polymer was immersed in fresh water for 20 s to remove weakly adhering analyte. Each polymer was combined with 1 ml of deionized water and placed in a 1 ml cuvette. The light absorbance of only the polymer (without the ITO or Si electrodes) was measured between a wavelength of 200 nm to 800 nm with a SmartSpec 3000 Spectrophotometer from Bio-Rad (Hercules, CA).

3.11 Statistical Analysis

3.11.1 Determination of Peak currents on Cyclic Voltammograms

The maximum (i_{pc}) and minimum (i_{pa}) peak currents at the oxidation-reductions shifts (Figure 2-4) on the cyclic voltammograms were selected for statistical analysis. The current ratio was the "peak current after addition of the analyte" to the "peak current before addition of the analyte" and was used to compare between cyclic voltammograms. All cyclic voltammograms were an average of three trials. Each trial was performed on a separate day using fresh solutions and new polymers to account for slight variations in the solutions and day-to-day error.

3.11.2 Evaluation of Blank and MIP Sensors

The equality of variances was tested on the absorbance values and current ratios using F-test prior to testing mean differences with t-test. T-test was performed on the absorbance values and mean current ratios to determine if the difference between the MIP and blank sensor was significant. The difference in the mean values was considered to be significant when the p-value was less than 0.05, representing a 95% confidence level.

3.12 Characterization of Surface

The surface of the MIP sensor was evaluated using atomic force microscopy (AFM). AFM experiments were performed with a NanoScope IIIa from Digital Instruments (Santa Barbara, CA) with the tapping mode. AFM images were obtained after template removal before rebinding and after template removal and rebinding. The removal of the template was performed for 1 h in 9:1 methanol/acetic acid. The rebinding was performed for 25 min in a 5 mM aqueous solution of theophylline. After rebinding, the sensor was immersed in clean water for 20 s to remove weakly adhering analyte.

CHAPTER 4: RESULTS AND DISCUSSION

4.1 Theory of Detection

The rebinding of the analyte to the imprinted polymer is observed through electrochemical measurements. The redox couple $Fe(CN)_6^{3-/4-}$ undergoes reasonably fast kinetics of electron transfer and was selected for this reason. The effect the rebinding of analyte to the MIP has upon this reversible reaction is monitored through measurement by cyclic voltammetry.

The current in the imprinted polymer is enhanced upon binding of the target analyte. Previous studies have shown an increase in current through potentiometric measurement (Yoshimi et al., 2001; Blanco-López et al., 2003b, 2003a). The reason for the increase in current upon binding of the analyte to the imprinted polymer is hypothesized to be due to the increase in the permeability of the polymer, called the shrinking effect (Figure 4-1). When the analyte binds in the imprinted sites, the polymer shrinks around the analyte, thereby increasing the size of the surrounding pores in the polymer. The increase in the pore size increases the permeability of the polymer and allows the charge to flow less restricted (Piletsky et al., 1996). The less restricted electron flow results in an increase in the measured current.

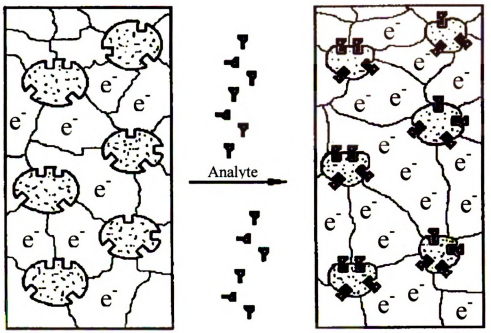

Figure 4-1. Schematic representation of the shrinking effect. Possible transformation in the arrangement of imprinted polymer upon rebinding of template molecule leading to increased electron flow (Adapted from Piletsky et al., 1996).

4.2 Confirmation of Imprinted Polymer

Theophylline at a concentration of 5 mM exhibited a maximum absorbance of 0.746 absorbance units (AU) at a wavelength of 295 nm (Data in Appendix A). Since the maximum absorbance for theophylline occurred at 295 nm, the absorbance of the non-imprinted polymer and MIP at this wavelength were used for further analysis.

The light absorbance values for the non-imprinted polymer and MIP at a wavelength of 295 nm were 0.038 ± 0.025 AU for the blank and 0.203 ± 0.055 AU for the MIP with a P-value of 0.018. The absorbance measurements of the non-imprinted

polymer compared to the MIP were significantly different at a 95% confidence level, indicating that an imprinted polymer was successfully formed for theophylline.

4.3 Characterization of Surface

The surface of the MIP was evaluated after template removal and after rebinding. The AFM image after template removal is shown in Figure 4-2 and the image after rebinding is displayed in Figure 4-3.

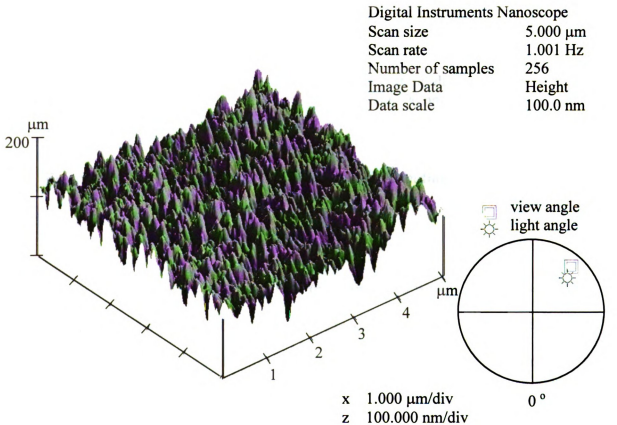

Figure 4-2. AFM image of MIP-ITO sensor after extraction of the theophylline template for 1 h in 9:1 methanol/acetic acid.

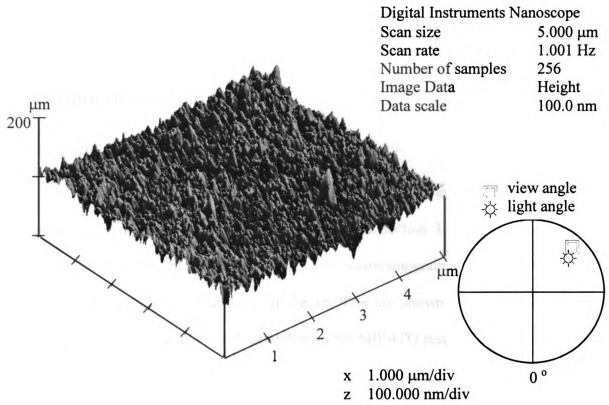

Figure 4-3. AFM image of MIP-ITO sensor after rebinding in 5 mM theophylline for 25 min.

The mean surface heights and standard deviations were 138.02 nm ± 17.735 nm for the MIP-ITO after extraction of the template and 95.522 nm ± 9.290 nm for the MIP-ITO after rebinding. The MIP-ITO after template extraction (Figure 4-2) is rougher than the MIP-ITO after rebinding (Figure 4-3). This can be observed visually from the images as well as by comparing the standard deviations of the heights. The standard deviation of the MIP-ITO after template extraction is almost two times greater than the standard deviation after rebinding. The decrease in the surface roughness upon analyte rebinding is hypothesized to be due to the shrinking effect. Upon rebinding of the target analyte,

the polymer shrinks around the analyte, thereby reducing the mean surface height and roughness of the polymer.

4.4 Initial Measurements – Cell A

4.4.1 MIP-ITO Sensor

The first measurements of the MIP-ITO sensor and MIP-Si sensor were performed with cell A. As previously discussed in section 3.4, the exposure area was circular with a diameter of 0.6 cm. The cyclic voltammograms of the B-ITO and MIP-ITO in the presence and absence of theophylline are shown in Figures 4-4 and 4-5, respectively. The addition of theophylline in the MIP-ITO resulted in an increase in the peak current of 0.036 mA. Addition of theophylline in the B-ITO resulted in a slight decrease in the peak current of 0.006. The ratio of the change in peak current after addition of theophylline for the MIP-ITO increased by a factor of six compared to the B-ITO.

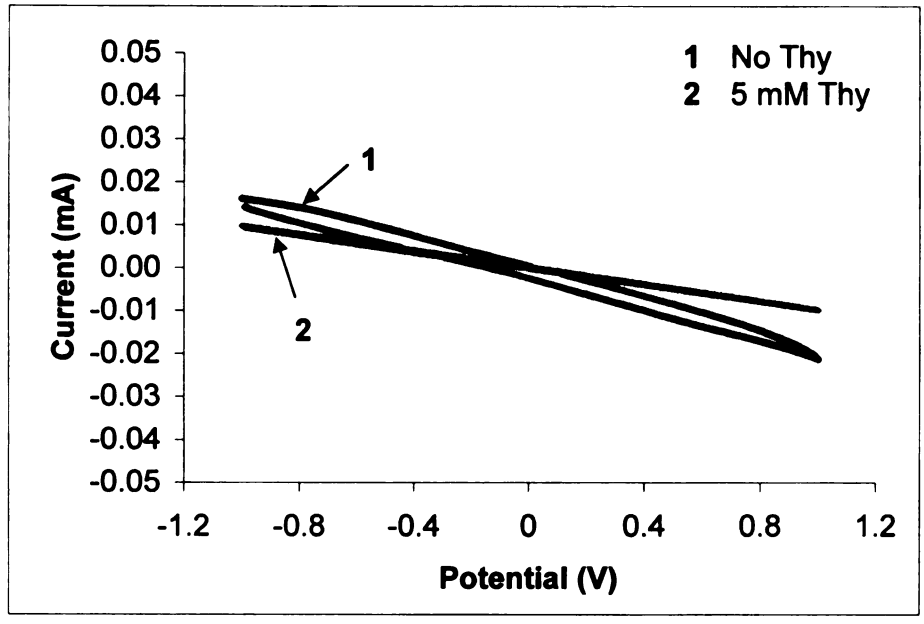

Figure 4-4. Cyclic voltammograms of B-ITO in the absence of theophylline and in 5 mM theophylline for cell A.

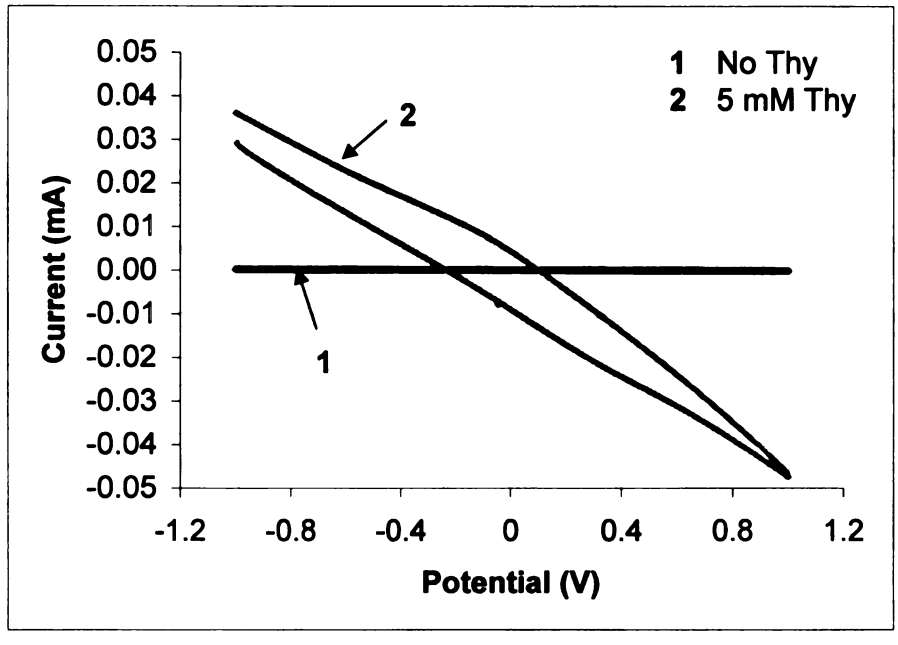

Figure 4-5. Cyclic voltammograms of MIP-ITO in the absence of theophylline and in 5 mM theophylline for cell A.

In a previous study by Yoshimi et al. (2001), ultraviolet radiation was used to induce polymerization. In this research, the MIP was polymerized thermally by the addition of heat. The bulk polymer was formed on the electrode and removed by breaking and subsequent washing steps. For removal of the template, Yoshimi et al. utilized sonication in water, while this research employed rinsing in a solution of methanol and acetic acid. Early trials in these experiments found that sonication removed the thin film polymer, which was confirmed through cyclic voltammetry. For this reason, sonication was rejected, and washing with an alcohol-acid solution was adapted.

4.4.2 MIP-Si Sensor

This research also conducted some initial tests of a thin MIP layer directly attached to silicon as a sensor. The initial measurements were performed in cell A, similar to the MIP-ITO sensor. The cyclic voltammograms for the B-Si and MIP-Si are shown in Figures 4-6 and 4-7, respectively. The change in the peak current before and after the addition of theophylline was 0.058 mA for the B-Si and 0.078 mA for the MIP-Si. The ratio of the changes in the peak current of the MIP-Si and the B-Si was only a factor of 1.3 and was not as marked as the six fold increase of the MIP-ITO to the B-ITO

The shapes of the curves for the silicon platform in Figures 4-6 and 4-7 are comparable to those on ITO shown in Figures 4-4 and 4-5. As in Figure 4-4 (B-ITO), the current response curve of B-Si before addition of theophylline is not flat compared to that of the MIP-Si. However, the response curve after addition of theophylline follows the curve before addition. This indicates that the response from B-Si is non-positive, because the difference between B-Si before and after addition of the analyte is small.

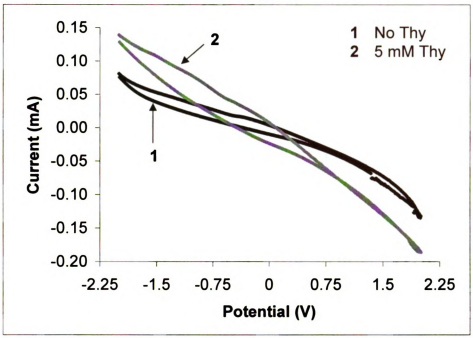

Figure 4-6. Cyclic voltammograms of B-Si in the absence of theophylline and 5 mM theophylline for cell A.

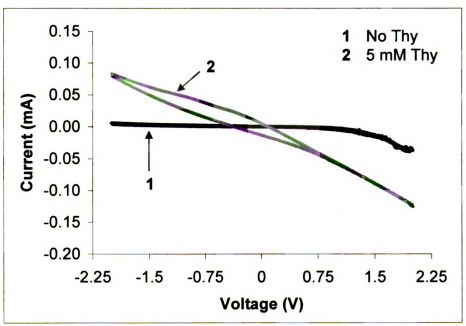

Figure 4-7. Cyclic voltammograms of MIP-Si in the absence of theophylline and 5 mM theophylline for cell A.

4.4.3 Comparison of peak currents for ITO and Silicon

The ratios of the peak currents of the MIP and non-imprinted polymer for ITO and silicon at the maximum and minimum potentials are shown in Tables 4-1 and 4-2, respectively. The standard deviations of 3 trials are included in the table as well as the P-value from performing a t-test on the B-ITO compared to the MIP-ITO on each material.

Table 4-1. Ratio of Maximum Currents (i_{pc}) of MIP and Blank on ITO and Silicon

Platform	Blank	MIP	P-Value
ITO	14.114 ± 23.177	74.408 ± 28.970	0.037
Silicon	1.169 ± 0.377	8.868 ± 7.027	0.008

Means ± standard deviations (n=3). Data was tested within a single row.

Table 4-2. Ratio of Minimum Currents (i_{pa}) of MIP and Blank on ITO and Silicon

Platform	Blank	MIP	P-Value
ITO	0.192 ± 1.043	62.364 ± 30.336	0.048
Silicon	2.131 ± 1.296	12.818 ± 3.507	0.131

Means ± standard deviations (n=3). Data was tested within a single row.

The increase in the ratio of the peak currents of the MIP-ITO compared to the B-ITO at a given potential showed that the MIP on ITO was successful. The ratios at the maximum potential were 74.4 and 14.1 for the MIP-ITO and B-ITO, respectively. The factor of increase between the MIP-ITO and B-ITO is 5.3 when only considering the maximum current. Yoshimi et al. (2001) found these ratios to be 2.94 for the MIP-ITO and 0.99 for the B-ITO with a factor of increase between the MIP and blank of three.

The increase in the ratio of the MIP to blank for this research compared to previous results might be attributed to the modification of the template removal procedure. The removal of the template by Yoshimi et al. was performed in water, while this research used a mixture of methanol and acetic acid. The alcohol-acid mixture was used in this research because of its prevalence for the removal of theophylline from a MAA-EGDMA copolymer (Vlatakis et al., 1993; Hong et al., 1998; Mullett and Lai, 1998). The template removal procedure will be investigated in a continuation of this research for its effectiveness as well as other factors that may contribute to the MIP signal, such as the thickness and uniformity of the MIP layer.

The ratios of the peak currents for silicon are shown for the MIP-Si and B-Si in Tables 4-1 and 4-2. These initial results demonstrated the potential for MIPs to be produced on a silicon electrode. The ratio of the peak currents increased by a factor of 7.5 for the MIP-Si compared to the B-Si at the maximum potential. The minimum currents were not considered because the means were not statistically different. The variation between different batches of MIPs on silicon merits further investigation to obtain a consistent response. Additional studies will be being conducted to increase the success of the theophylline MIP on silicon.

MIPs immobilized on silicon show potential for research. Silicon is a relatively inexpensive material whose properties can be uniquely and precisely controlled (Zhang, 2001). Previous literature has shown difficulty forming a thin MIP layer on silicon (Hedborg et al., 1993). The potential for research into MIPs attached to silicon will likely increase because few studies have been conducted, and many possibilities for MIP sensors still exist.

The initial results of this research were conducted with cell A, where the working electrode was at the bottom of the electrochemical cell. The inconsistent results obtained with cell A were hypothesized to be due to contact area between the working electrode and the copper plate where the alligator clip was attached (refer to Figure 3-1). Because the ITO layer was only on one side of the glass slide, there was no direct connection from the ITO layer to the potentiostat. The glass slide acted as a barrier and interfered with the signal from the sensor. Due to the this issue, electrochemical cell B was used for all further testing because the sensor (working electrode) was directly connected to the potentiostat through the contact between the ITO layer and the alligator clip. In addition to the improved connectivity, cell B was also used because the measurements were occurring over a greater surface area.

4.5 Sensitivity and Selectivity Testing Measurements of Submerged Working Electrode – Cell B

4.5.1 Background Measurement

The cyclic voltammogram of the background measurement of 5 mM potassium ferrocyanide and 0.1 M potassium nitrate with 5 mM theophylline is shown in Figure 4-8. The working electrode was cleaned, untreated ITO (no silanization or polymer). The

presence of theophylline does not alter the shape of the cyclic voltammogram compared to a typical voltammogram in Figure 2-4.

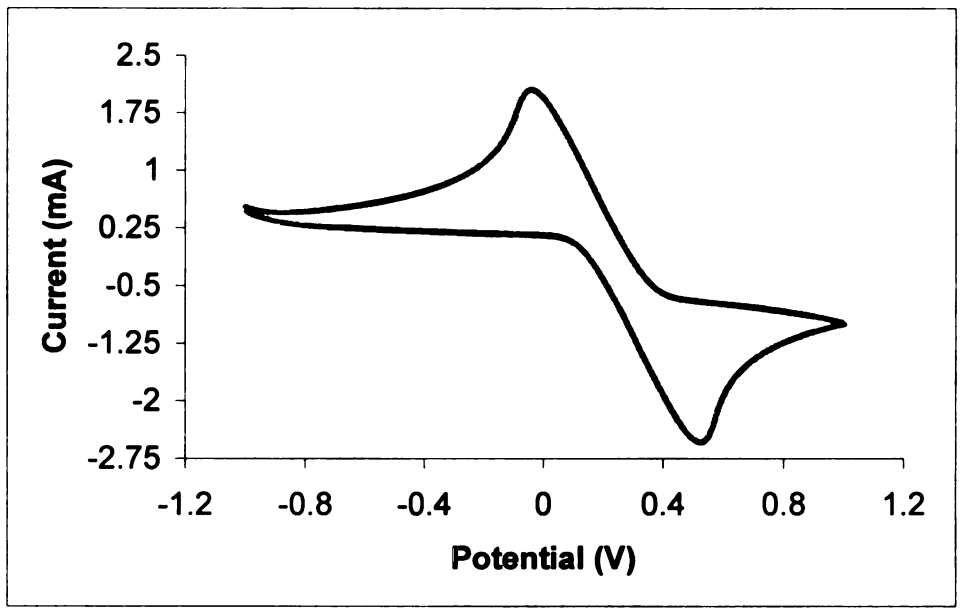

Figure 4-8. Cyclic voltammogram of 5 mM potassium ferrocyanide and 0.1 M potassium nitrate with 5 mM theophylline on untreated ITO.

4.5.2 Sensitivity of MIP-ITO Sensor

The sensitivity of the MIP-ITO sensor was evaluated using the fully submerged cell (cell B). This electrochemical cell was used to improve the sensitivity. The submersion of the working electrode in cell B was hypothesized to give a higher signal than cell A due to the increased surface area of the ITO electrode and the MIP. Cell B was selected for the sensitivity measurements due to the increased surface area. The surface area of cell B was approximately 1 cm^2 while the surface area of cell A was only 0.28 cm^2 (diameter of 0.6 cm). Furthermore, cell B was used for the selectivity testing

because the shape of the background measurements in cell B resembled those of a typical cyclic voltammogram (Figure 4-8 compared to Figure 2-4).

The sensitivity of the MIP-ITO sensor was evaluated by testing the response at 4 analyte concentrations: 1, 2, 3, and 4 mM. The cyclic voltammograms of the B-ITO and MIP-ITO sensor in the presence and absence of various analyte concentrations are shown in Figures 4-9 to 4-16. The response before addition of the analyte served as a baseline for evaluating the response of each sensor. For this reason, the response of each sensor to the analyte was compared to the baseline measurement. This allowed the sensors to be compared and evaluated, and accounted for any slight differences in conductivity that may have been present between samples.

The results obtained with cell B did not have as large an increase in the signal as was the case for cell A. Measurements with cell B were still explored due to the overall increase in current and because the shape of the cyclic voltammogram resembled that of a typical curve in Figure 2-4.

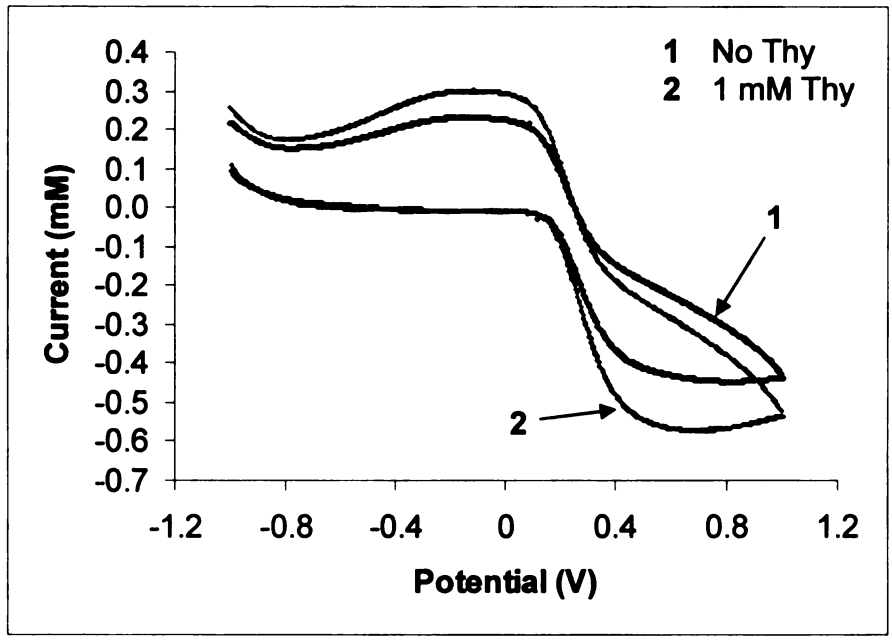

Figure 4-9. Cyclic voltammogram of B-ITO sensor evaluated at 1 mM theophylline.

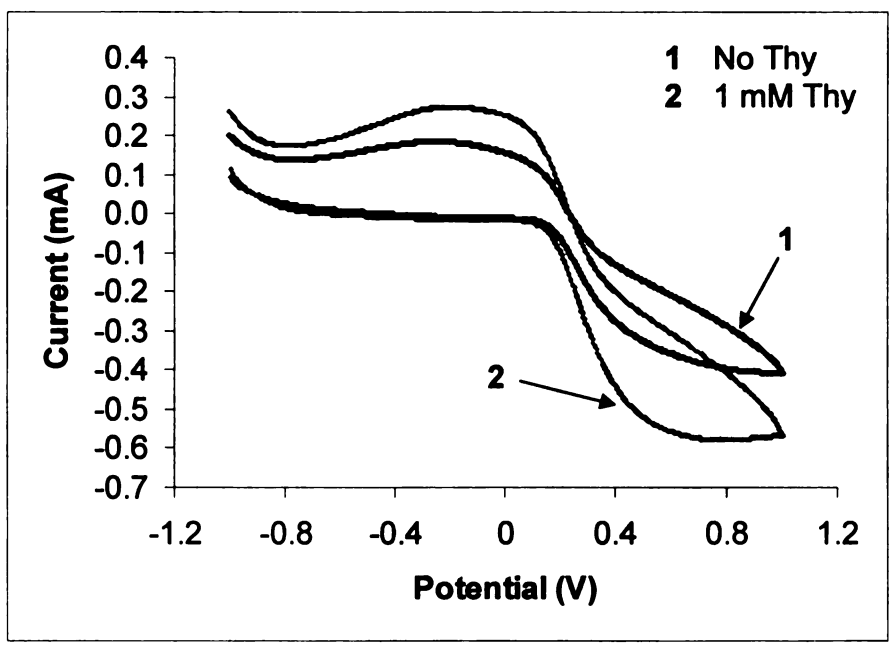

Figure 4-10. Cyclic voltammogram of MIP-ITO sensor evaluated at 1 mM theophylline.

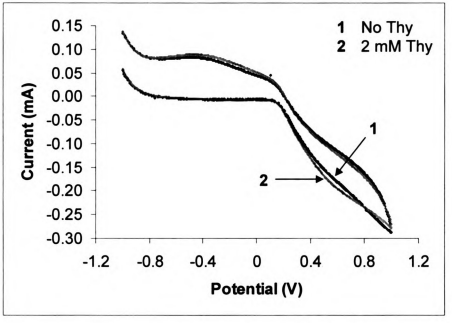

Figure 4-11. Cyclic voltammogram of B-ITO sensor evaluated at 2 mM theophylline.

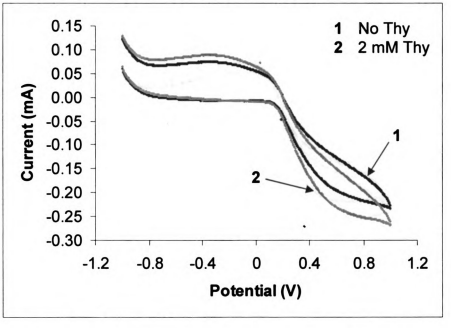

Figure 4-12. Cyclic voltammogram of MIP-ITO sensor evaluated at 2 mM theophylline.

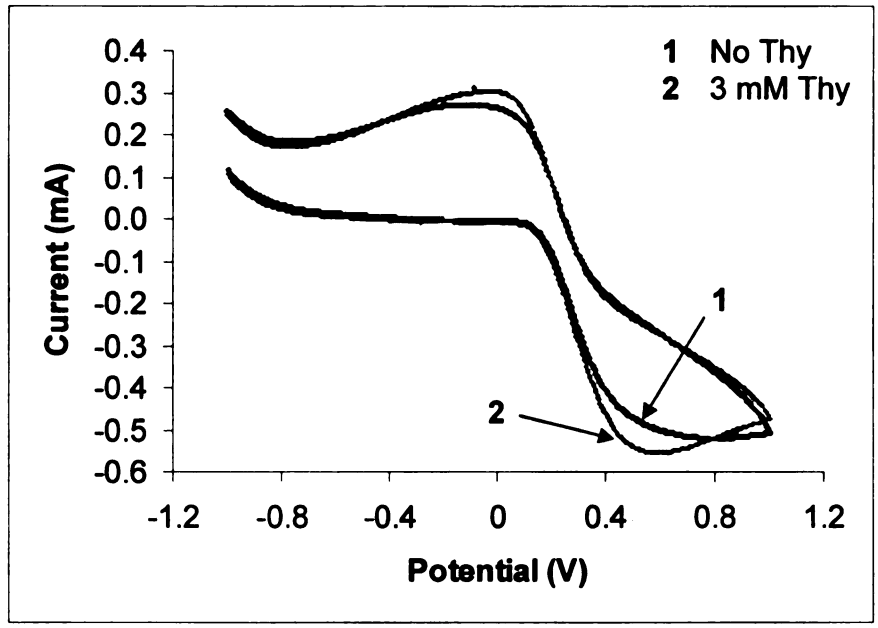

Figure 4-13. Cyclic voltammogram of B-ITO sensor evaluated at 3 mM theophylline.

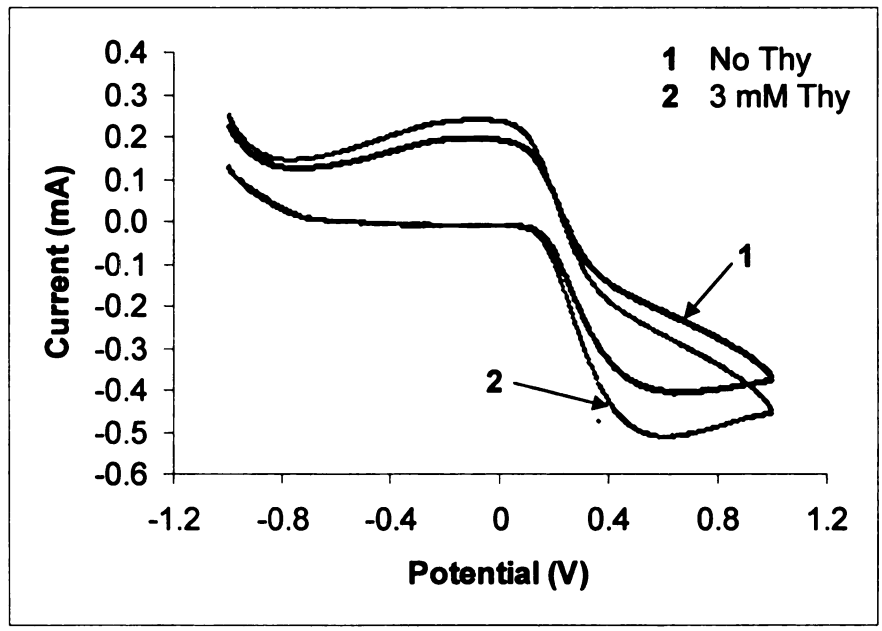

Figure 4-14. Cyclic voltammogram of MIP-ITO sensor evaluated at 3 mM theophylline.

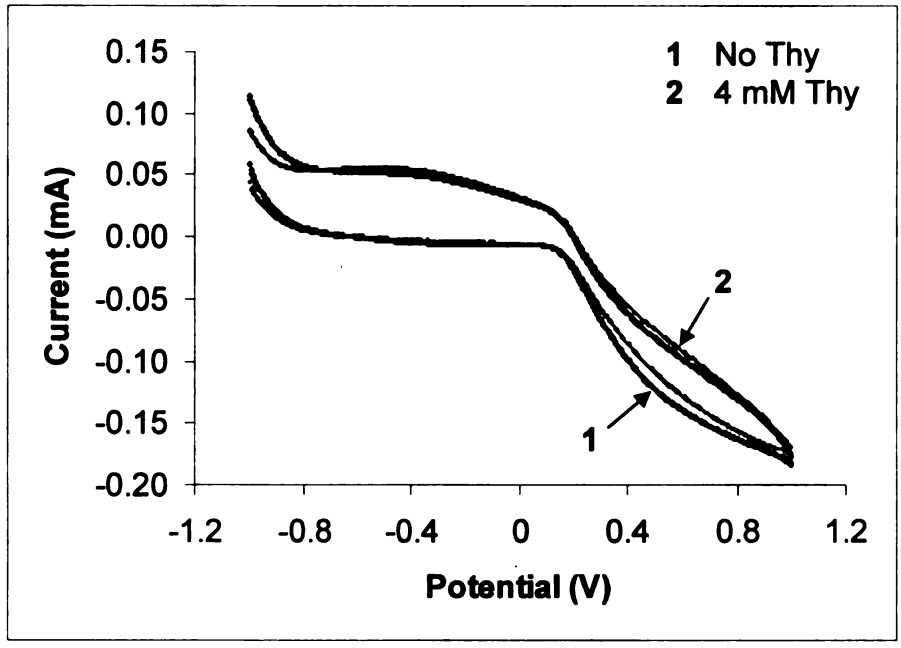

Figure 4-15. Cyclic voltammogram of B-ITO sensor evaluated at 4 mM theophylline.

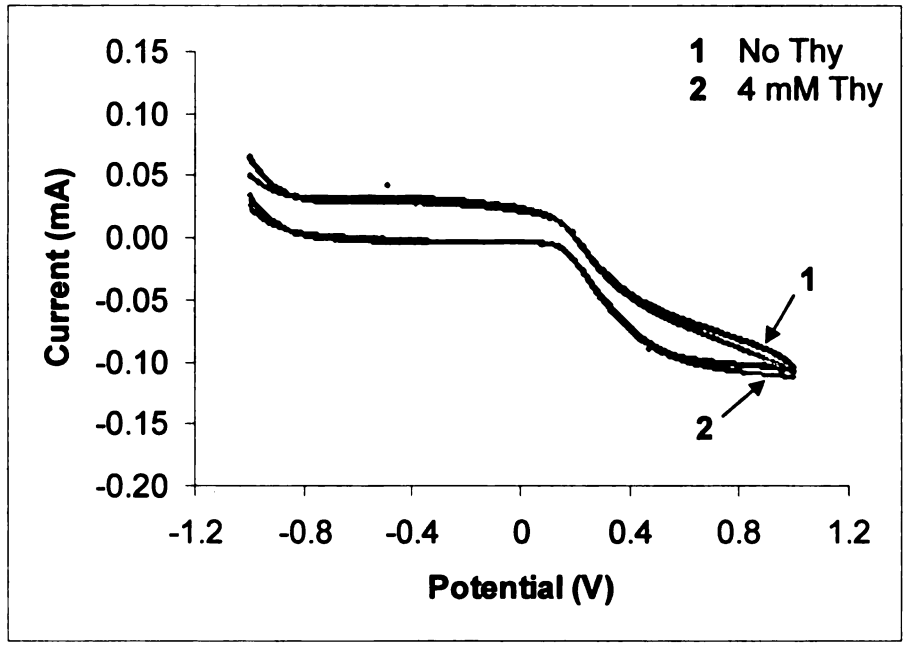

Figure 4-16. Cyclic voltammogram of MIP-ITO sensor evaluated at 4 mM theophylline

The ratio of the maximum (i_{pc}) and minimum (i_{pa}) peak currents for 1, 2, 3, and 4 mM theophylline are shown in Tables 4-3 and 4-4, respectively. The ratio refers to the peak current on the curve of the selected concentration (1, 2, 3, or 4 mM Thy) divided by the peak current on the baseline curve without theophylline (no Thy). The resulting p-values using t-test are shown in the tables for each concentration that was tested.

Table 4-3. Ratio of Maximum Currents (i_{pc}) of B-ITO and MIP-ITO Sensors at Various Analyte Concentrations

Analyte Concentration	B-ITO	MIP-ITO	P-Value
1 mM Thy	1.022 ± 0.058	1.418 ± 0.347	0.123
2 mM Thy	1.073 ± 0.075	1.223 ± 0.054	0.049
3 mM Thy	1.139 ± 0.142	1.659 ± 0.169	0.015
4 mM Thy	1.024 ± 0.026	1.188 ± 0.115	0.074

Means ± standard deviations (n=3). Data was tested within a row (one concentration).

Table 4-4. Ratio of Minimum Currents (i_{pa}) of B-ITO and MIP-ITO Sensors at Various Analyte Concentrations

Analyte Concentration	B-ITO	MIP-ITO	P-Value
1 mM Thy	1.055 ± 0.152	1.413 ± 0.368	0.217
2 mM Thy	1.093 ± 0.136	1.196 ± 0.129	0.393
3 mM Thy	1.126 ± 0.181	1.515 ± 0.203	0.068
4 mM Thy	0.926 ± 0.152	1.327 ± 0.575	0.363

Means ± standard deviations (n=3). Data was tested within a row (one concentration).

The ratio of the maximum currents was compared for the B-ITO and the MIP-ITO sensors at each analyte concentration. The currents ratios (max or min) were not significantly different for the 1 mM theophylline concentration. The ratio of the maximum currents was significantly different ($P<0.05$) at a theophylline concentration of 2 mM, but not significant at the minimum current. When testing was performed with 3 mM theophylline, the ratio of the maximum currents was significantly different ($P<0.05$), and the ratio of the minimum currents tended to significance (P-value of 0.068). The ratio of maximum currents at a concentration of 4 mM tended to significance (P-value of 0.074).

The MIP-ITO sensor could detect the theophylline analyte in the range of 2 to 4 mM. The optimum concentration of theophylline for detection was 3 mM, which resulted in the highest P-value between the B-ITO and MIP-ITO.

The maximum currents were used for evaluating the sensitivity of the MIP-ITO sensor. This was the region where the most current would flow based upon the increase in the permeability and highest number of free electrons that would be present. In this research, the current at a single potential was used to evaluate the success or failure of each sensor. Future researchers may consider other analysis techniques such as principal component analysis or some type of modeling method to determine what region of data on the cyclic voltammogram should be compared for increased examination of the results.

A graphical comparison of the current ratios between the MIP-ITO and B-ITO is presented in Figure 4-17. The MIP-ITO sensor was able to significantly detect the analyte at concentrations between 2 to 4 mM theophylline. The ratio of currents at 3 mM theophylline yielded the lowest P-value. Therefore, the optimum analyte concentration found in this study was 3 mM theophylline.

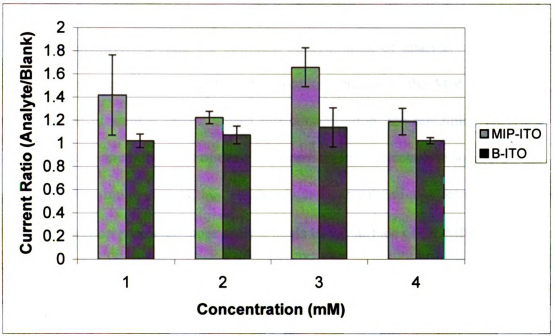

Figure 4-17. Comparison of the ratio of maximum currents of MIP-ITO sensor to B-ITO at various analyte concentrations.

Theophylline is a small bronchodilator drug that is used in the treatment of asthma, bronchitis, emphysema, and other airways diseases. The amount needed in the blood to relieve airway constriction is between 5 to 15 μg/ml (National Jewish Medical and Research Center, 2005). The sensitivity of the MIP-ITO sensor was between 2 to 4 mM theophylline, which was 360 to 900 μg/ml when converted into units used for the

monitoring of theophylline. The current sensitivity target would be to make the biomimetic sensor able to detect theophylline in the 5 to 15 μg/ml range needed for delivery and monitoring.

The hook effect has been well established in immunoassay sensors (Rodbard et al., 1978; Amarasiri Fernando and Wilson, 1992) and states that at higher analyte concentrations, the over abundance of analyte may interfere rather than enhance the signal. The hook effect may be present in the MIP-ITO sensor and would account for the decline in sensitivity around the optimum concentration of analyte. At the optimum concentration, most of the analyte in the solution rebinds to the MIP surface. As the concentration of analyte increases past this concentration, the remaining analyte in the solution hinders the movement of the charge carriers in the electrolyte solution.

The maximum current, i_{pc}, yields a higher current and a better signal because as the redox reaction proceeds, more analyte binds to the surface of the MIP. As previously described, the permeability of the polymer is thought to increase as more analyte binds to the surface. The increased permeability results in more electron transfer, thus yielding a higher signal.

4.5.3 Selectivity of MIP-ITO Sensor

The selectivity of the sensor was tested using the structurally related molecule caffeine. The cyclic voltammograms for the MIP-ITO sensor tested at concentrations of 1, 2, 3, and 4 mM caffeine are shown in Figures 4-18 to 4-25.

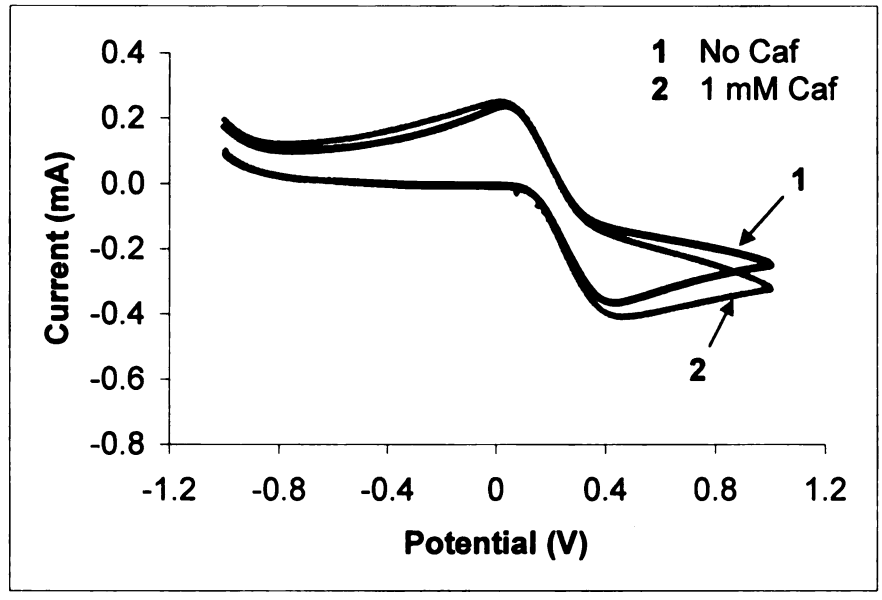

Figure 4-18. Cyclic voltammogram of B-ITO sensor evaluated at 1 mM caffeine.

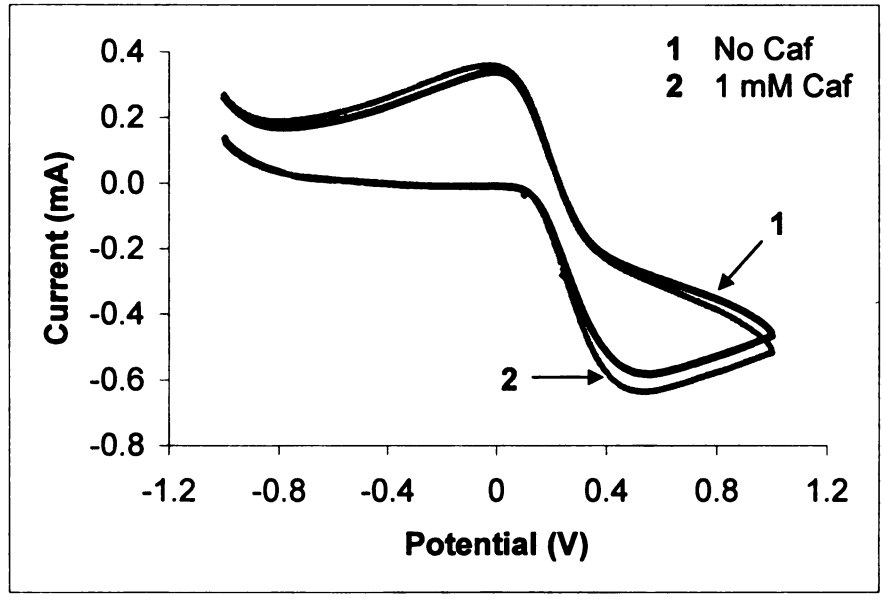

Figure 4-19. Cyclic voltammogram of MIP-ITO sensor evaluated at 1 mM caffeine.

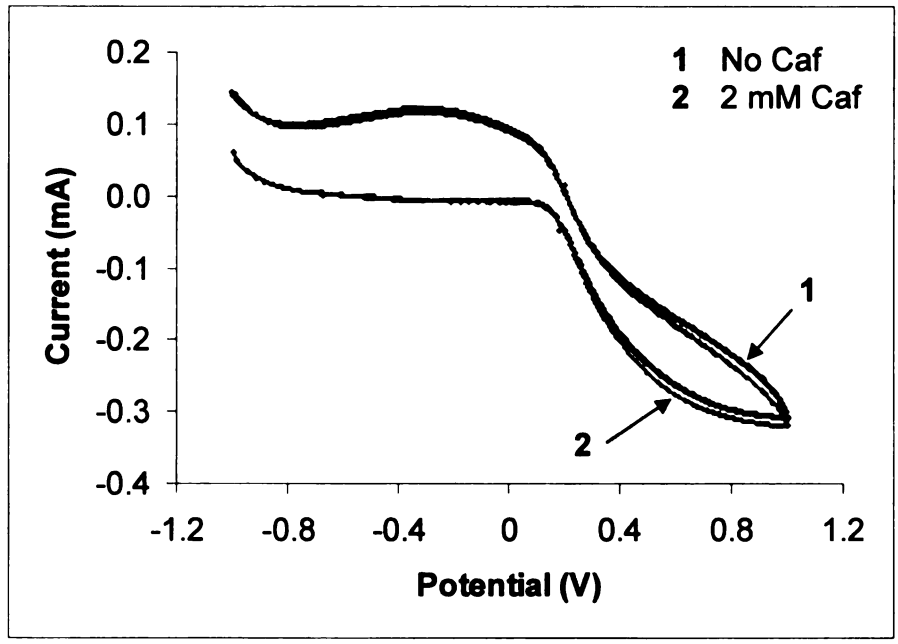

Figure 4-20. Cyclic voltammogram of B-ITO sensor evaluated at 2 mM caffeine.

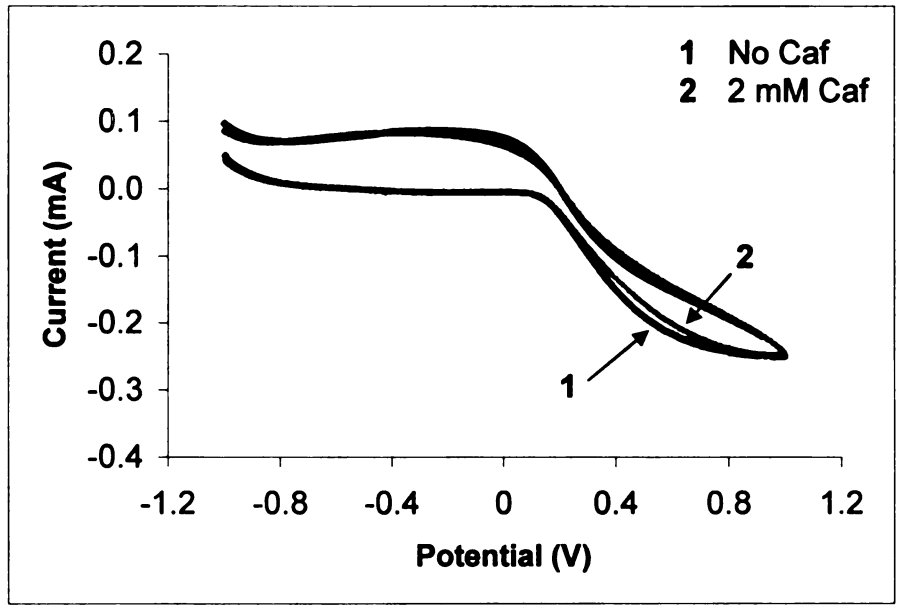

Figure 4-21. Cyclic voltammogram of MIP-ITO sensor evaluated at 2 mM caffeine.

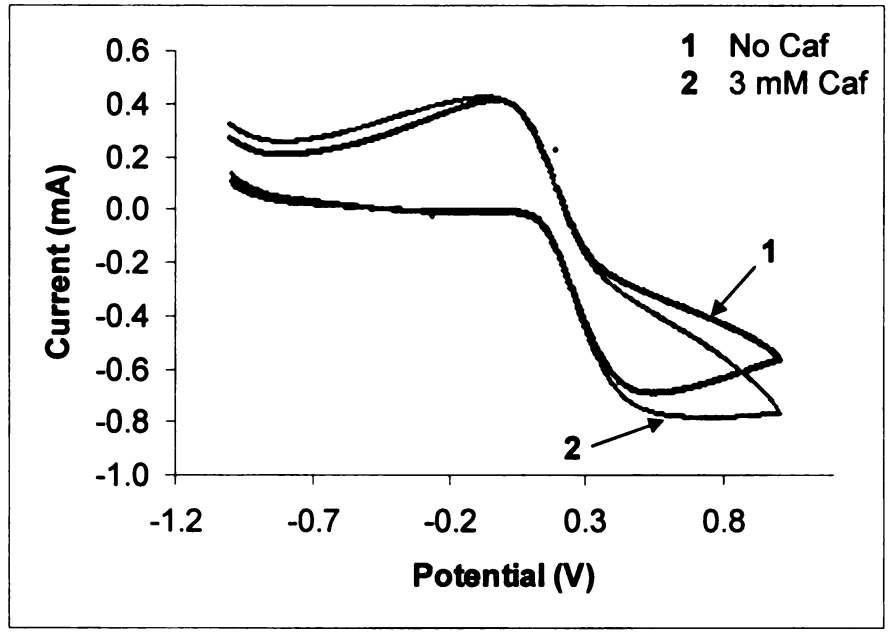

Figure 4-22. Cyclic voltammogram of B-ITO sensor evaluated at 3 mM caffeine.

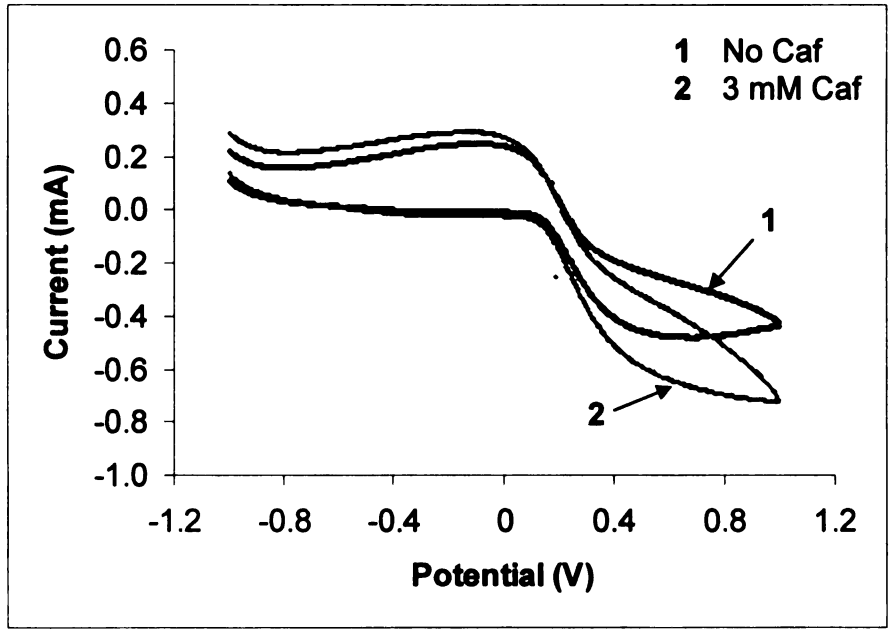

Figure 4-23. Cyclic voltammogram of MIP-ITO sensor evaluated at 3 mM caffeine.

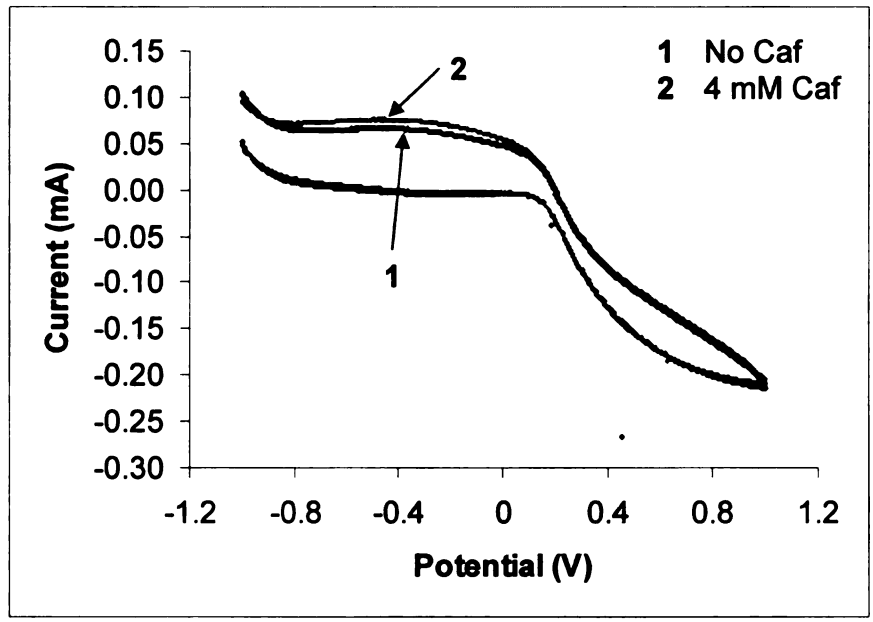

Figure 4-24. Cyclic voltammogram of B-ITO sensor evaluated at 4 mM caffeine.

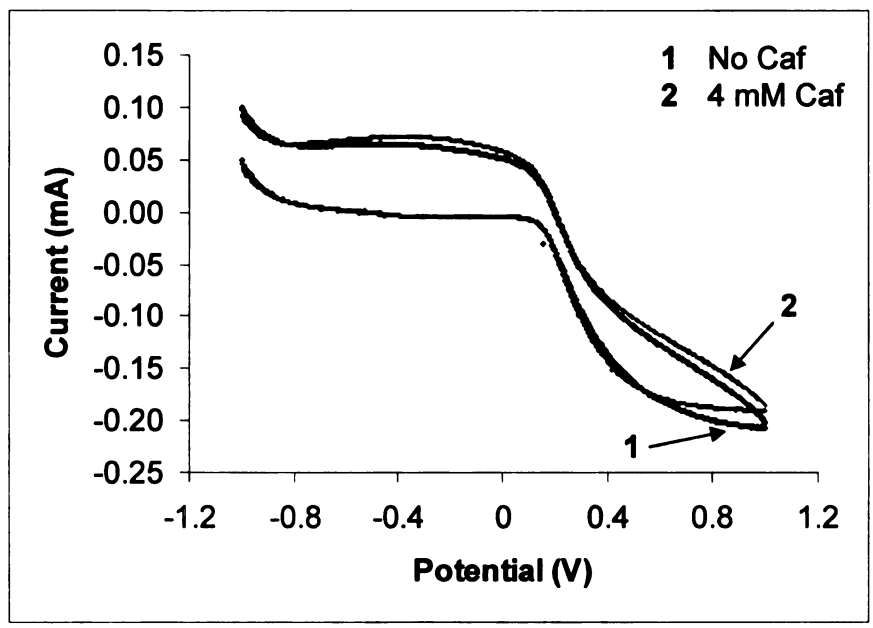

Figure 4-25. Cyclic voltammogram of MIP-ITO sensor evaluated at 4 mM caffeine.

The MIP-ITO sensor and B-ITO did not show a marked response at any concentration of caffeine. The current ratios of the B-ITO and MIP-ITO at the maximum and minimum currents are shown in Tables 4-5 and 4-6, respectively. The mean current ratios and standard deviations are presented in the tables. The maximum current ratios of the B-ITO were compared to the MIP-ITO to determine the selectivity of the biomimetic sensor.

Table 4-5. Ratio of Maximum Currents (i_{pc}) of B-ITO and MIP-ITO Sensor at Various Counter Analyte Concentrations

Counter-Analyte Concentration	B-ITO	MIP-ITO	P-Value
1 mM Caf	1.403 ± 0.350	1.130 ± 0.265	0.343
2 mM Caf	1.172 ± 0.217	1.065 ± 0.236	0.595
3 mM Caf	1.250 ± 0.452	1.473 ± 0.721	0.681
4 mM Caf	1.169 ± 0.111	0.970 ± 0.092	0.075

Means ± standard deviations (n=3). Data was tested within a row (one concentration).

Table 4-6. Ratio of Minimum Currents (i_{pa}) of B-ITO and MIP-ITO Sensor at Various Counter Analyte Concentrations

Counter-Analyte Concentration	B-ITO	MIP-ITO	P-Value
1 mM Caf	1.516 ± 0.530	1.068 ± 0.134	0.229
2 mM Caf	1.139 ± 0.190	1.028 ± 0.098	0.419
3 mM Caf	1.525 ± 0.861	2.020 ± 1.62	0.672
4 mM Caf	1.329 ± 0.502	1.025 ± 0.575	0.419

Means ± standard deviations (n=3). Data was tested within a row (one concentration).

The differences in the mean currents ratios (maximum and minimum) for the B-ITO and MIP-ITO were not significant at a 95% confidence level when tested for selectivity. The p-values of the biomimetic sensor compared to the blank sensor were all greater than 0.05 when the sensor was tested with caffeine. The biomimetic sensor did not show any response to caffeine at the tested concentrations; therefore, the sensor was selective to the target analyte, theophylline.

4.6 Selection of Future Compound for Food Safety

Patulin is a mycotoxin that may be found in a variety of foods such as grain, fruit, and cheese (chemical structure found in Figure 4-26). It is produced by certain species of the *Penicillium*, *Aspergillus*, and *Byssochylamys* molds and is primarily of concern in apples and apples products. The current action level for patulin set by the Food and Drug Administration is 50 μg/kg (FDA, 2000). Patulin is a good candidate for molecular imprinting due to its small chemical structure and the large number of polar groups able to interact with a functional monomer.

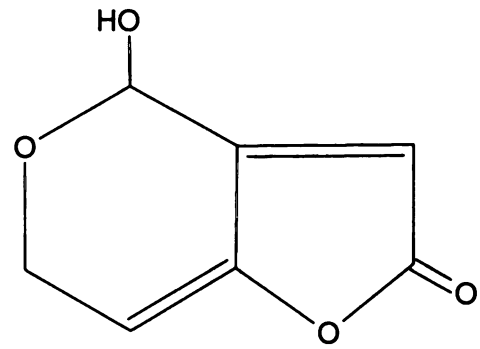

Figure 4-26. Chemical structure of patulin (Sigma-Aldrich, 2004).

An initial experiment for the mycotoxin patulin is shown in Figure 4-27. The procedure was modified due to the high cost of the toxin (Appendix C-3). Briefly, the rebinding and measurement procedures for patulin were modified by submerging the sample into a known concentration of analyte followed by measurement in electrochemical cell A. Due to the change in procedure, the graph only shows two curves, one for the patulin-imprinted electrode and the non-imprinted polymer. The following results show only one replicate.

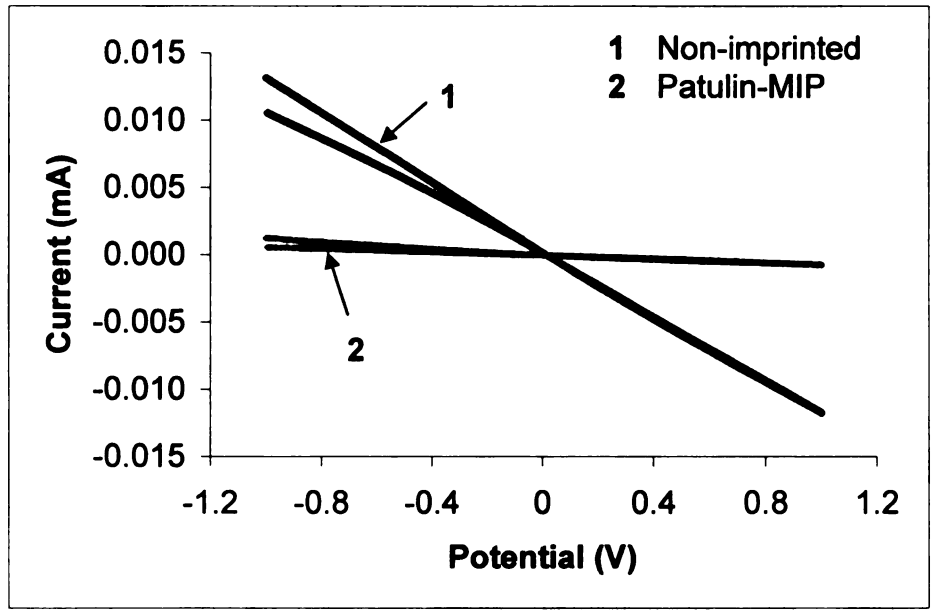

Figure 4-27. Initial cyclic voltammogram for patulin MIP.

The current for the non-imprinted curve (1) is greater than the patulin MIP (2). This trend was not observed with the theophylline MIP, where the current was consistently larger for the MIP than the blank polymer. This may have been due to the change in the procedure or to the interaction between patulin and the MIP upon rebinding. Additional experimentation will be necessary to investigate these results and determine their consistency.

Patulin will continue to be of interest in the area of food safety. Current detection methods use a liquid-liquid extraction of patulin with ethyl acetate to remove it from the sample followed by detection and quantification, usually by HPLC (Dombrink-Kurtzman, 2005). The identification of patulin through antibody-based detection methods is being investigated due to the speed and sensitivity of immunological procedures. However, the low molecular weight of patulin (154 g/mol) makes it difficult to generate antibodies without conjugation to a protein (McElroy and Weiss, 1993; Sheu et al., 1999). Investigation into rapid MIP-based sensors for patulin will be essential to food safety because of the difficulty of producing antibodies and the processing for current detection methods.

CHAPTER 5: CONCLUSIONS

5.1 General Conclusions

This research demonstrated the successful formation of a MIP and its attachment to an electrode. The successful formation of the MIP and attachment to indium tin oxide (ITO) was monitored by AFM imaging. The initial results of the theophylline MIP on ITO supported the findings of a previous study (Yoshimi et al.) using the same MIP and template. The presence of theophylline in the initial study increased the maximum peak current by a factor of 5.3 for the MIP-ITO sensor compared to the blank or non-imprinted polymer (omission of theophylline). The increase in the peak current in the presence of the analyte (a rise of 0.006 mA for B-ITO and 0.036 mA for MIP-ITO) allowed the system to act as a qualitative sensor to the presence of theophylline.

The sensitivity and selectivity of the MIP-ITO sensor was successfully evaluated. The biomimetic sensor was able to detect the theophylline analyte between concentrations of 2 mM to 4 mM. The optimum analyte concentration was 3 mM theophylline. The MIP-ITO sensor showed no cross reactivity to caffeine at concentrations of 2 mM to 4 mM and, therefore, was selective to theophylline. Initial studies of the MIP on silicon found the ratio of maximum currents to increase by a factor of 7.5 when comparing the MIP-Si to the B-Si. The MIP on silicon was able to detect the analyte at the 5 mM concentration.

5.2 Recommendations for Future Research

The ability to control the thickness of the MIP may be important to obtaining a uniform signal. Additional research should be performed to control the thickness and uniformity of the polymer, such as a spin coating method. Reducing the thicknesses of the polymer may increase the sensitivity of the sensor. Future investigation into a monolayer of polymer may be useful to evaluate the maximum sensitivity of the sensor.

Additional testing would also help to evaluate the effect of other stressing conditions on the response of the MIP sensor, such as high temperatures, acidic and basic conditions, and long storage times. It may be useful to determine or measure the density of the analyte in the polymer or MIP pockets. This may be critical for determining the amount of residual analyte trapped in the polymer matrix, which could be affecting the response of the biomimetic sensor.

In addition to the improvements that can be made to the MIP on ITO, the response of the MIP on silicon may be further improved by modifying the surface characteristics of silicon. One test that may be tried is to increase the conductivity by using silicon that is more highly doped with charges. The higher current may promote enhanced rebinding of the analyte. Various surface profiles, such as porous structures, could be investigated for their effect upon the resulting signal. The method of detection may also affect the signal. Other detection techniques may be investigated to obtain an optimal signal, such as various pulse voltammetry techniques (normal, differential, square wave, or staircase).

The biomimetic sensor for theophylline should be improved to achieve the sensitivities necessary to compete with current detection methods. The preceding recommendations for improvement to the sensor will allow the detection range to reach 5

to 15 μg/ml needed by the medical industry. Once the sensitivity is increased to the needs of industry, the stability and simplicity of the sensor will allow it to compete with other detection methods for theophylline.

The final aim of this research was to assess and recommend a toxin for study in the area of food safety. The mycotoxin patulin was suggested for future research. This research may lead to a sensor that would detect patulin and other toxins, improving food safety. Future studies should target small toxins where natural receptors are difficult to obtain or are unavailable.

REFERENCES

Aherne, A., C. Alexander, M. J. Payne, N. Perez, and E. N. Vulfson. 1996. Bacteria-mediated lithography of polymer surfaces. *J. Am. Chem. Soc.* 118(36): 8771-8772.

Alocilja, E. C., and S. M. Radke. 2003. Market analysis of biosensors for food safety. *Biosensors and Bioelectronics.* 18(5-6): 841-846.

Amarasiri Fernando, S., and G. S. Wilson. 1992. Studies of the 'hook' effect in the one-step sandwich immunoassay. *Journal of Immunological Methods.* 151(1-2): 47-66.

Andersson, L., B. Sellergren, and Mosbach, Klaus. 1984. Imprinting of amino acid derivatives in macroporous polymers. *Tetrahedron Letters.* 25(45): 5211-5214.

Andersson, L. I. 1996. Application of molecular imprinting to the development of aqueous buffer and organic solvent based radioligand binding assays for (S)-Propranolol. *Analytical Chemistry.* 68(1): 111-117.

Baggiani, C., G. Giraudi, and A. Vanni. 2002. A molecular imprinted polymer with recognition properties towards the carcinogenic mycotoxin ochratoxin A. *Bioseparation.* 10(6): 389-394.

Baggiani, C., F. Trotta, G. Giraudi, C. Giovannolia, and A. Vannia. 1999. A molecularly imprinted polymer for the pesticide bentazone. *Analytical Communications.* 36(7): 263-266.

Bard, A. J., and L. R. Faulkner. 2000. *Electrochemical methods : fundamentals and applications*. 2nd ed. New York: John Wiley.

Blanco-Lopez, M. C., M. J. Lobo-Castanon, A. J. Miranda-Ordieres, and P. Tunon-Blanco. 2004. Electrochemical sensors based on molecularly imprinted polymers. *TrAC Trends in Analytical Chemistry.* 23(1): 36-48.

Blanco-López, M. C., M. J. Lobo-Castañón, A. J. Miranda-Ordieres, and P. Tuñón-Blanco. 2003a. Voltammetric response of diclofenac-molecularly imprinted film modified carbon electrodes. *Anal Bioanal Chem.* 377: 257-261.

Blanco-López, M. C., M. J. Lobo-Castañón, A. J. Miranda-Ordieres, and P. Tuñón-Blanco. 2003b. Voltammetric sensor for vanillylmandelic acid based on molecularly imprinted polymer-modified electrodes. *Biosensors and Bioelectronics.* 18(4): 353-362.

Chen, G. H., Z. B. Guan, C. T. Chen, L. T. Fu, V. Sundaresan, and F. H. Arnold. 1997. A glucose-sensing polymer. *Nature Biotechnology.* 15(4): 354-357.

Chianella, I., M. Lotierzo, S. A. Piletsky, I. E. Tothill, B. Chen, K. Karim, and A. P. F. Turner. 2002. Rational design of a polymer specific for microcystin-LR using a computational approach. *Analytical Chemistry.* 74(6): 1288-1293.

Das, K., J. Penelle, and V. Rotello. 2003. Selective picomolar detection of hexachlorobenzene in water using a quartz crystal microbalance coated with a molecularly imprinted polymer thin film. *Langmuir.* 19(9): 3921-3925.

Dickert, F. L., and O. Hayden. 1999. Imprinting with sensor development-on the way to synthetic antibodies. *Fresenius Journal of Analytical Chemistry.* 364: 506-511.

Dombrink-Kurtzman, M. A. 2005. *Methods For Detecting And Quantifying Patulin In Apple Products*: Crc Press.

Duffy, D. J., K. Das, S. L. Hsu, J. Penelle, V. M. Rotello, and H. D. Stidham. 2002. Binding efficiency and transport properties of molecularly imprinted polymer thin films. *Journal of the American Chemical Society.* 124(28): 8290-8296.

Fairhurst, R. E., C. Chassaing, R. F. Venn, and A. G. Mayes. 2004. A direct comparison of the performance of ground, beaded and silica-grafted MIPs in HPLC and Turbulent Flow Chromatography applications. *Biosensors and Bioelectronics.* 20(6): 1098-1105.

FDA. Center for Food Safety and Applied Nutrition. 2000. Patulin in Apple Juice, Apple Juice Concentrates and Apple Juice Products. http://vm.cfsan.fda.gov/~dms/patubckg.html. Accessed on November 26, 2004.

Haupt, K., and K. Mosbach. 2000. Molecularly imprinted polymers and their use in biomimetic sensors. *Chem. Rev.* 100(7): 2495-2504.

Hedborg, E., F. Winquist, I. Lundstrom, L. I. Andersson, and K. Mosbach. 1993. Some studies of molecularly-imprinted polymer membranes in combination with field-effect devices. *Sensors and Actuators A: Physical.* 37-38: 796-799.

Hong, J.-M., P. E. Anderson, J. Qian, and C. R. Martin. 1998. Selectively-permeable ultrathin film composite membranes based on molecularly-imprinted polymer. *Chem. Mater.* 10(4): 1029-1033.

Iqbal, S. S., M. F. Lulka, J. P. Chambers, R. G. Thompson, and J. J. Valdes. 2000. Artificial receptors: molecular imprints discern closely related toxins. *Materials Science and Engineering: C.* 7(2): 77-81.

Jakoby, B., G. M. Ismail, M. P. Byfield, and M. J. Vellekoop. 1999. A novel molecularly imprinted thin film applied to a Love wave gas sensor. *Sensors and Actuators A: Physical.* 76(1-3): 93-97.

Jenkins, A. L., R. Yin, and J. L. Jensen. 2001. Molecularly imprinted polymer sensors for pesticide and insecticide detection in water. *The Analyst.* 126(6): 798-802.

Jodlbauer, J., N. M. Maier, and W. Lindner. 2002. Towards ochratoxin A selective molecularly imprinted polymers for solid-phase extraction. *Journal of Chromatography A.* 945: 45-63.

Kempe, M. 1996. Antibody-mimicking polymers as chiral stationary phases in HPLC. *Analytical Chemistry.* 68(11): 1948-1953.

Kriz, D., M. Kempe, and K. Mosbach. 1996. Introduction of molecularly imprinted polymers as recognition elements in conductometric chemical sensors. *Sensors and Actuators B: Chemical.* 33(1-3): 178-181.

Kriz, D., C. B. Kriz, L. I. Andersson, and K. Mosbach. 1994. Thin-layer chromatography based on the molecular imprinting technique. *Analytical Chemistry.* 66(17): 2636-2639.

Kroger, S., A. P. Turner, K. Mosbach, and K. Haupt. 1999. Imprinted polymer-based sensor system for herbicides using differential-pulse voltammetry on screen-printed electrodes. *Analytical Chemistry.* 71(17): 3698-3702.

Lai, E. P. C., A. Fafara, V. A. VanderNoot, M. Kono, and B. Polsky. 1998. Surface plasmon resonance sensors using molecularly imprinted polymers for sorbent assay of theophylline, caffeine, and xanthine. *Canadian Journal of Chemistry.* 76(3): 265-273.

Liang, C., H. Peng, X. Bao, L. Nie, and S. Yao. 1999. Study of a molecular imprinting polymer coated BAW bio-mimic sensor and its application to the determination of caffeine in human serum and urine. *The Analyst.* 124(12): 1781–1785.

Lu, Y., C. Li, X. Liu, and W. Huang. 2002. Molecular recognition through the exact placement of functional groups on non-covalent molecularly imprinted polymers. *Journal of Chromatography A.* 950: 89-97.

Lulka, M. F., S. S. Iqbal, J. P. Chambers, E. R. Valdes, R. G. Thompson, M. T. Goode, and J. J. Valdes. 2000. Molecular imprinting of Ricin and its A and B chains to organic silanes: fluorescence detection. *Materials Science & Engineering C - Biomimetic and Supramolecular Systems.* 11(2): 101-105.

Malitesta, C., I. Losito, and P. G. Zambonin. 1999. Molecularly imprinted electrosynthesized polymers: new materials for biomimetic sensors. *Analytical Chemistry.* 71(7): 1366-1370.

Mayes, A. G., and K. Mosbach. 1997. Molecularly imprinted polymers: useful materials for analytical chemistry? *TrAC Trends in Analytical Chemistry.* 16(6): 321-332.

McElroy, L. J., and C. M. Weiss. 1993. The production of polyclonal antibodies against the mycotoxin derivative patulin hemiglutarate. *Canadian Journal of Microbiology.* 39(9): 861-863.

Merkoçi, A., and S. Alegret. 2002. New materials for electrochemical sensing IV. Molecular imprinted polymers. *Trends in Analytical Chemistry.* 21(11): 717-725.

Muhammad-Tahir, Z., and E. C. Alocilja. 2003. A conductometric biosensor for biosecurity. *Biosensors and Bioelectronics.* 18(5-6): 813-819.

Muhammad-Tahir, Z., and E. C. Alocilja. 2004. A Disposable Biosensor for Pathogen Detection in Fresh Produce Samples. *Biosystems Engineering.* 88(2): 145-151.

Mullett, W. M., and E. P. C. Lai. 1998. Determination of theophylline in serum by molecularly imprinted solid-phase extraction with pulsed elution. *Analytical Chemistry.* 70(17): 3636-3641.

National Jewish Medical and Research Center. 2005. Theophylline: Questions and answers. http://www.nationaljewish.org/medfacts/theo.html. Accessed on November 3, 2005.

Panasyuk-Delaney, T., V. M. Mirsky, M. Ulbricht, and O. S. Wolfbeis. 2001. Impedometric herbicide chemosensors based on molecularly imprinted polymers. *Analytica Chimica Acta.* 435(1): 157-162.

Pérez-Moral, N., and A. G. Mayes. 2002. Novel MIP formats. *Bioseparation.* 10(6): 287-299.

Piletsky, S. A., S. Alcock, and A. P. F. Turner. 2001a. Molecular imprinting: at the edge of the third millennium. *Trends in Biotechnology.* 19(1): 9-12.

Piletsky, S. A., E. V. Piletskaya, T. A. Sergeyeva, T. L. Panasyuk, and A. V. El'skaya. 1999. Molecularly imprinted self-assembled films with specificity to cholesterol. *Sensors and Actuators B: Chemical.* 60(2-3): 216-220.

Piletsky, S. A., E. V. Piletskaya, K. Yano, A. Kugimiya, A. V. Elgersma, R. Levi, U. Kahlow, T. Takeuchi, and I. Karube. 1996. A biomimetic receptor system for sialic acid based on molecular imprinting. *Analytical Letters.* 29(2): 157-170.

Piletsky, S. A., S. Subrahmanyam, and A. P. F. Turner. 2001b. Application of molecularly imprinted polymers in sensors for the environment and biotechnology. *Sensor Review.* 21(4): 292-296.

Pine Instrument Company. Survey of three voltammetric methods. http://www.pineinst.com/ecweb/academia/expt3.htm. Accessed on October 28, 2004.

Radke, S. M., and E. C. Alocilja. 2005. A high density microelectrode array biosensor for detection of E. coli O157:H7. *Biosensors and Bioelectronics.* 20(8): 1662-1667.

Ramström, O., K. Skudar, J. Haines, P. Patel, and O. Brüggemann. 2001. Food analyses using molecularly imprinted polymers. *Journal of Agricultural and Food Chemistry.* 49(5): 2105-2114.

Rashid, B. A., R. J. Briggs, J. N. Hay, and D. Stevenson. 1997. Preliminary evaluation of a molecular imprinted polymer for solid-phase extraction of tamoxifen. *Analytical Communications.* 34(10): 303-306.

Rodbard, D., Y. Feldman, M. L. Jaffe, and L. E. M. Miles. 1978. Kinetics of two-site immunoradiometric ('sandwich') assays--II : Studies on the nature of the -high-dose hook effect. *Molecular Immunology.* 15(2): 77-82.

Sergeyeva, T. A., S. A. Piletsky, A. A. Brovko, E. A. Slinchenko, L. M. Sergeeva, and A. V. El'skaya. 1999. Selective recognition of atrazine by molecularly imprinted polymer membranes. Development of conductometric sensor for herbicides detection. *Analytica Chimica Acta.* 392(2-3): 105-111.

Sheu, F., O. Lee, and Y. T. Shyu. 1999. The synthesis of antigens and the product of antibodies against patulin derivatives. *Journal of Food and Drug Analysis.* 7(1): 65-72.

Sigma-Aldrich. 2004. *Sigma Biochemicals & Reagents for Life Science Research.* 2004-2005 ed. 1531.

Stevenson, D. 1999. Molecular imprinted polymers for solid-phase extraction. *TrAC Trends in Analytical Chemistry.* 18(3): 154-158.

Suarez-Rodriguez, J. L., and M. E. Diaz-Garcia. 2000. Flavonol fluorescent flow-through sensing based on a molecular imprinted polymer. *Analytica Chimica Acta.* 405(1-2): 67-76.

Subrahmanyam, S., S. A. Piletsky, E. V. Piletska, B. Chen, K. Karim, and A. P. F. Turner. 2001. 'Bite-and-switch' approach using computationally designed molecularly imprinted polymers for sensing of creatinine. *Biosensors and Bioelectronics.* 16(9-12): 631-637.

Surugiu, I., B. Danielsson, L. Ye, K. Mosbach, and K. Haupt. 2001a. Chemiluminescence imaging ELISA using an imprinted polymer as the recognition element instead of an antibody. *Analytical Chemistry.* 73(3): 487-491.

Surugiu, L., J. Svitel, L. Ye, K. Haupt, and B. Danielsson. 2001b. Development of a flow injection capillary chemiluminescent ELISA using an imprinted polymer instead of the antibody. *Analytical Chemistry.* 73(17): 4388-4392.

Svenson, J., and I. A. Nicholls. 2001. On the thermal and chemical stability of molecularly imprinted polymers. *Analytica Chimica Acta.* 435(1): 19-24.

Takeuchi, T., D. Fukuma, and J. Matsui. 1999. Combinatorial molecular imprinting: an approach to synthetic polymer receptors. *Anal. Chem.* 71(2): 285-290.

Tamayo, F. G., M. M. Titirici, A. Martin-Esteban, and B. Sellergren. Synthesis and evaluation of new propazine-imprinted polymer formats for use as stationary phases in liquid chromatography. *Analytica Chimica Acta.* In Press, Corrected Proof.

Tan, Y., H. Peng, C. Liang, and S. Yao. 2001. A new assay system for phenacetin using biomimic bulk acoustic wave sensor with a molecularly imprinted polymer coating. *Sensors and Actuators B: Chemical.* 73(2-3): 179-184.

Vlatakis, G., L. I. Andersson, R. Müller, and K. Mosbach. 1993. Drug assay using antibody mimics made by molecular imprinting. *Nature.* 361: 645-647.

Wang, J. 2000. *Analytical Electrochemistry.* Second ed. New York: Wiley-VCH.

Weiss, R., M. Freudenschuss, R. Krska, and B. Mizaikoff. 2003. Improving methods of analysis for mycotoxins: molecularly imprinted polymers for deoxynivalenol and zearalenone. *Food Additives And Contaminants.* 20(4): 386-395.

Whitcombe, M. J., M. E. Rodriguez, P. Villar, and E. N. Vulfson. 1995. A new method for the introduction of recognition site functionality into polymers prepared by molecular imprinting: synthesis and characterization of polymeric receptors for cholesterol. *Journal of the American Chemical Society.* 117(27): 7105-7111.

Wulff, G., A. Sarhan, and K. Zabrocki. 1973. Enzyme-analogue built polymers and their use for the resolution of racemates. *Tetrahedron Letters.* 14(44): 4329-4332.

Wulff, G. 2002. Enzyme-like catalysis by molecularly imprinted polymers. *Chemical Reviews.* 102(1): 1-28.

Yan, M., and A. Kapua. 2001. Fabrication of molecularly imprinted polymer microstructures. *Analytica Chimica Acta.* 435(1): 163-167.

Yano, K., and I. Karube. 1999. Molecularly imprinted polymers for biosensor applications. *TrAC Trends in Analytical Chemistry.* 18(3): 199-204.

Yoshimi, Y., R. Ohdaira, C. Iiyama, and K. Sakai. 2001. "Gate effect" of thin layer of molecularly-imprinted poly(methacrylic acid-co-ethyleneglycol dimethacrylate). *Sensors and Actuators B: Chemical.* 73(1): 49-53.

Zhang, X. G. 2001. *Electrochemistry of Silicon and Its Oxide*. New York: Kluwer Academic/Plenum Publishers.

Zhu, Q.-Z., K. Haupt, D. Knopp, and R. Niessner. 2002. Molecularly imprinted polymer for metsulfuron-methyl and its binding characteristics for sulfonylurea herbicides. *Analytica Chimica Acta.* 468(2): 217-227.

APPENDICES

Appendix A: Light Absorbance Tables and Raw Data

Table A-1. Light Absorbance Values for Aqueous 5mM Theophylline.

Polymer Sample	Absorbance (AU)
1	0.731
2	0.753
3	0.753

Table A-2. Light Absorbance Values for Non-imprinted Polymer.

Sample	Absorbance Before Rebinding (AU)	Absorbance After Rebinding (AU)	Difference
1	0.12	0.175	0.055
2	0.15	0.2	0.05
3	0.04	0.05	0.01

Table A-3. Light Absorbance Values for MIP.

Sample	Absorbance Before Rebinding (AU)	Absorbance After Rebinding (AU)	Difference
1	0.08	0.245	0.165
2	0.142	0.321	0.179
3	0.179	0.445	0.266

Table A-4. Comparison of Light Absorbance Difference of MIP to Non-imprinted Polymer Using t-Test for Two Samples Assuming Unequal Variances.

	Variable 1	*Variable 2*
Mean	0.038333333	0.203333333
Variance	0.000608333	0.002994333
Observations	3	3
Hypothesized Mean Difference	0	
df	3	
t Stat	-4.761376574	
P(T<=t) one-tail	0.008795191	
t Critical one-tail	2.353363016	
P(T<=t) two-tail	0.017590382	
t Critical two-tail	3.182449291	

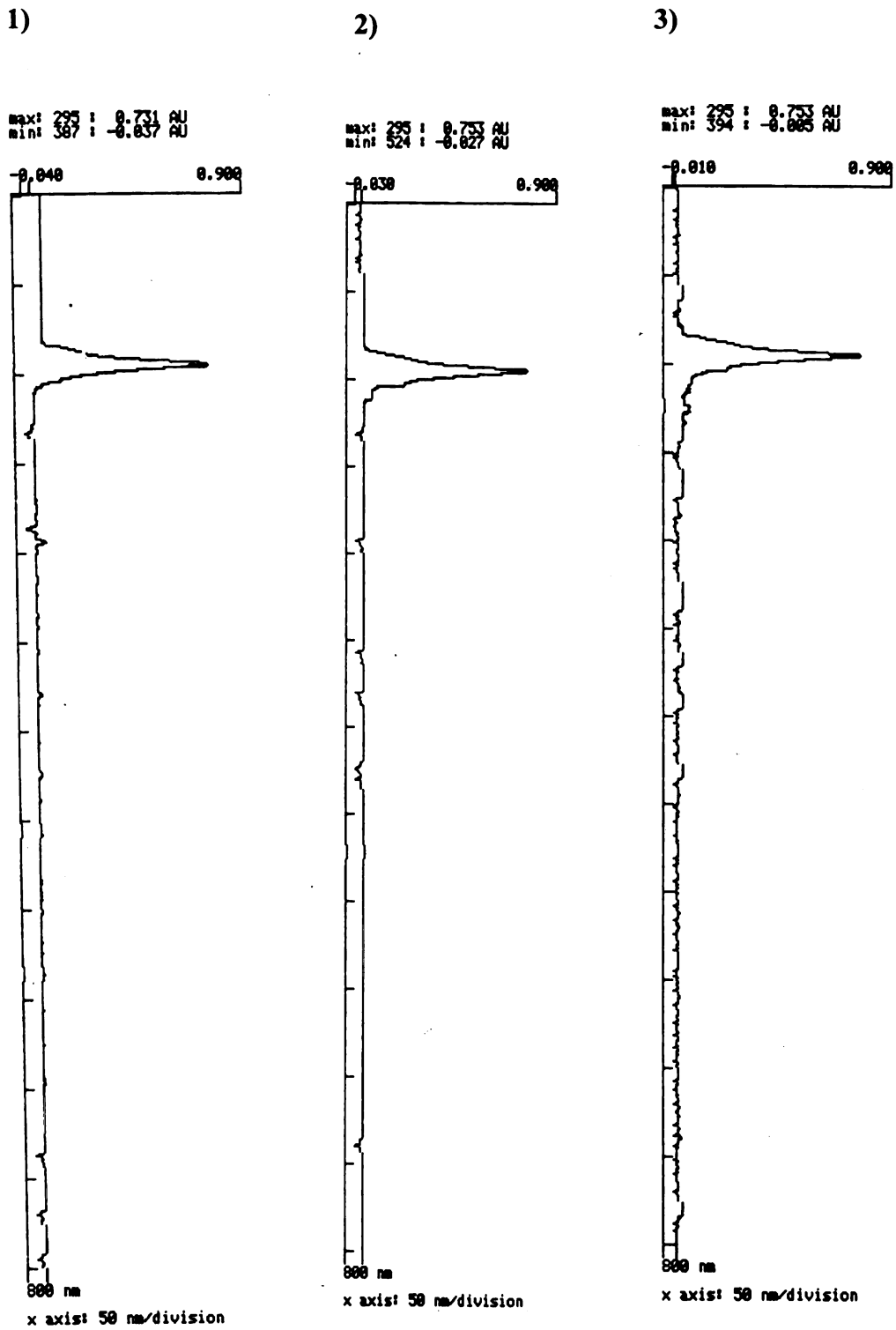

Figure A-1. Light absorbance data for an aqueous solution of 5 mM theophylline.

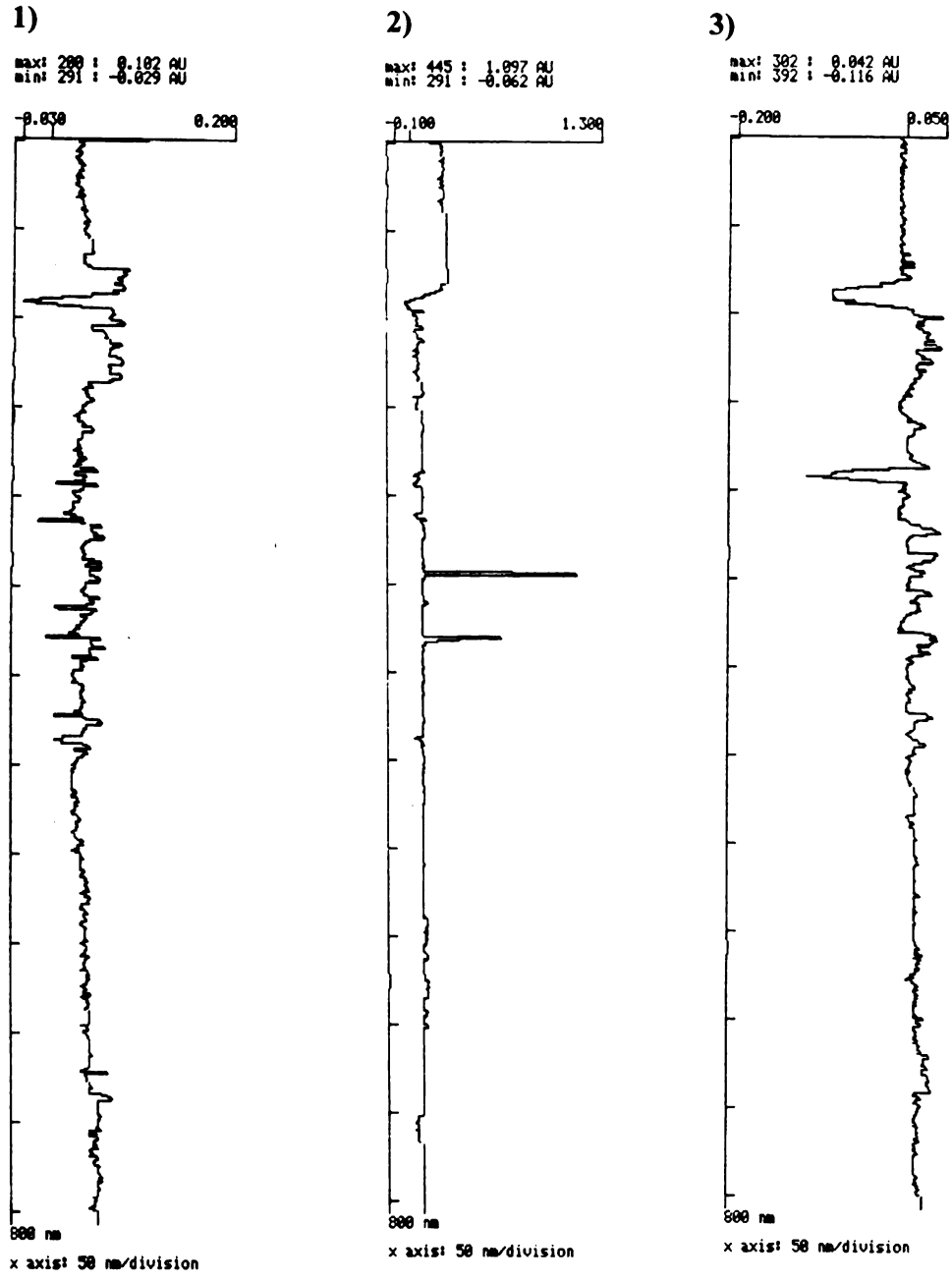

Figure A-2. Light absorbance data for non-imprinted polymer after extraction of template.

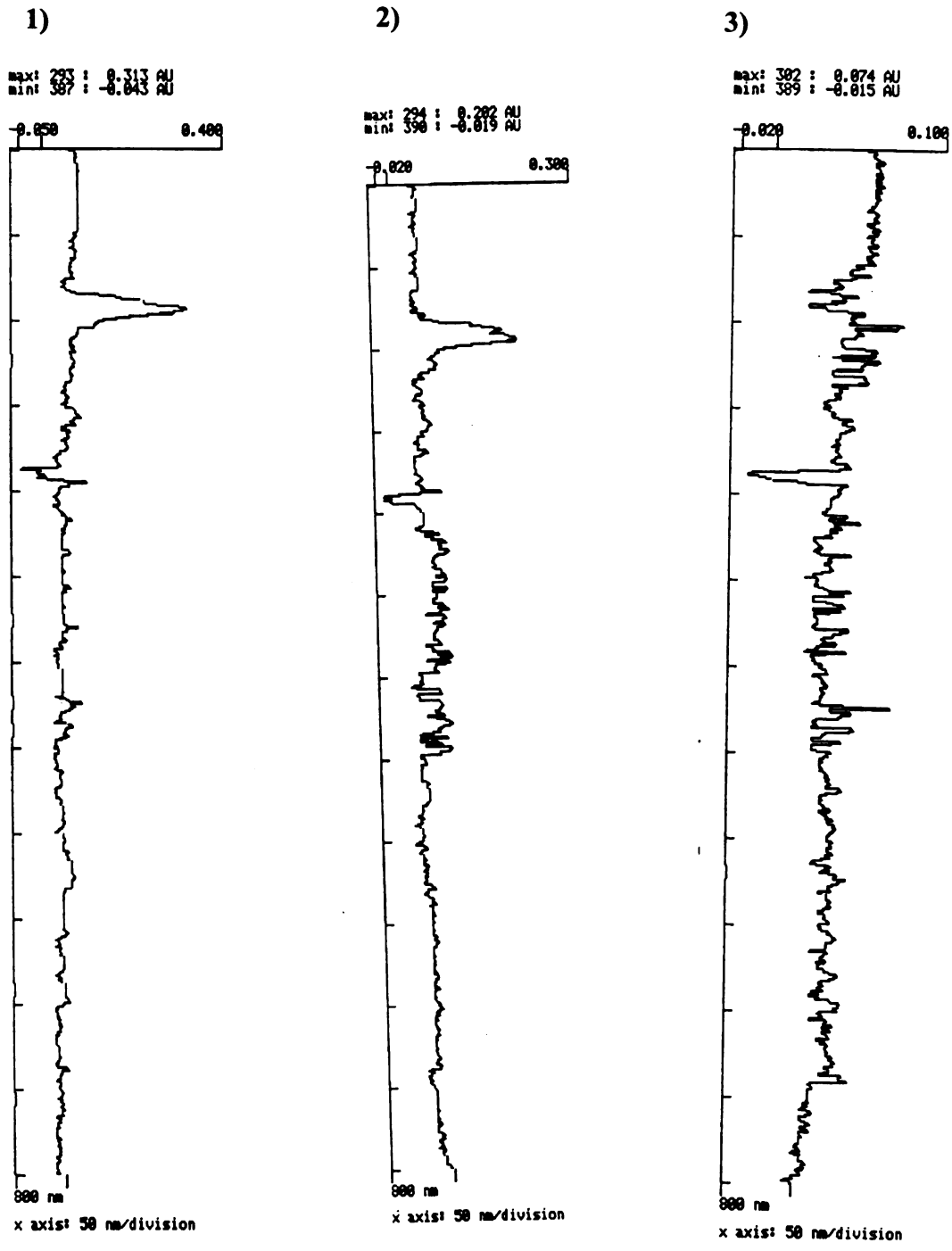

Figure A-3. Light absorbance data for non-imprinted polymer after soaking 25min in an aqueous solution of 5 mM theophylline.

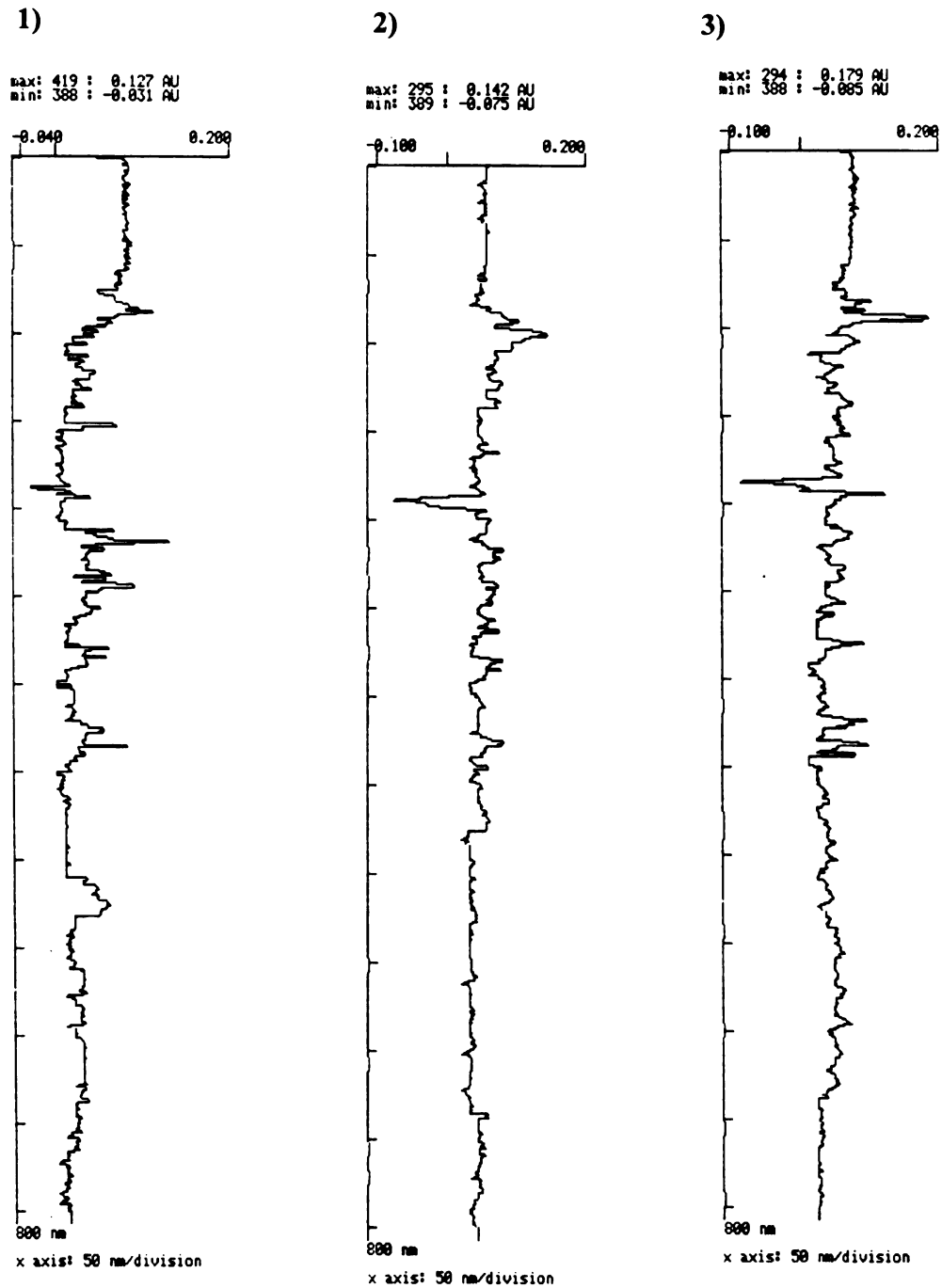

Figure A-4. Light absorbance data for MIP after extraction of template.

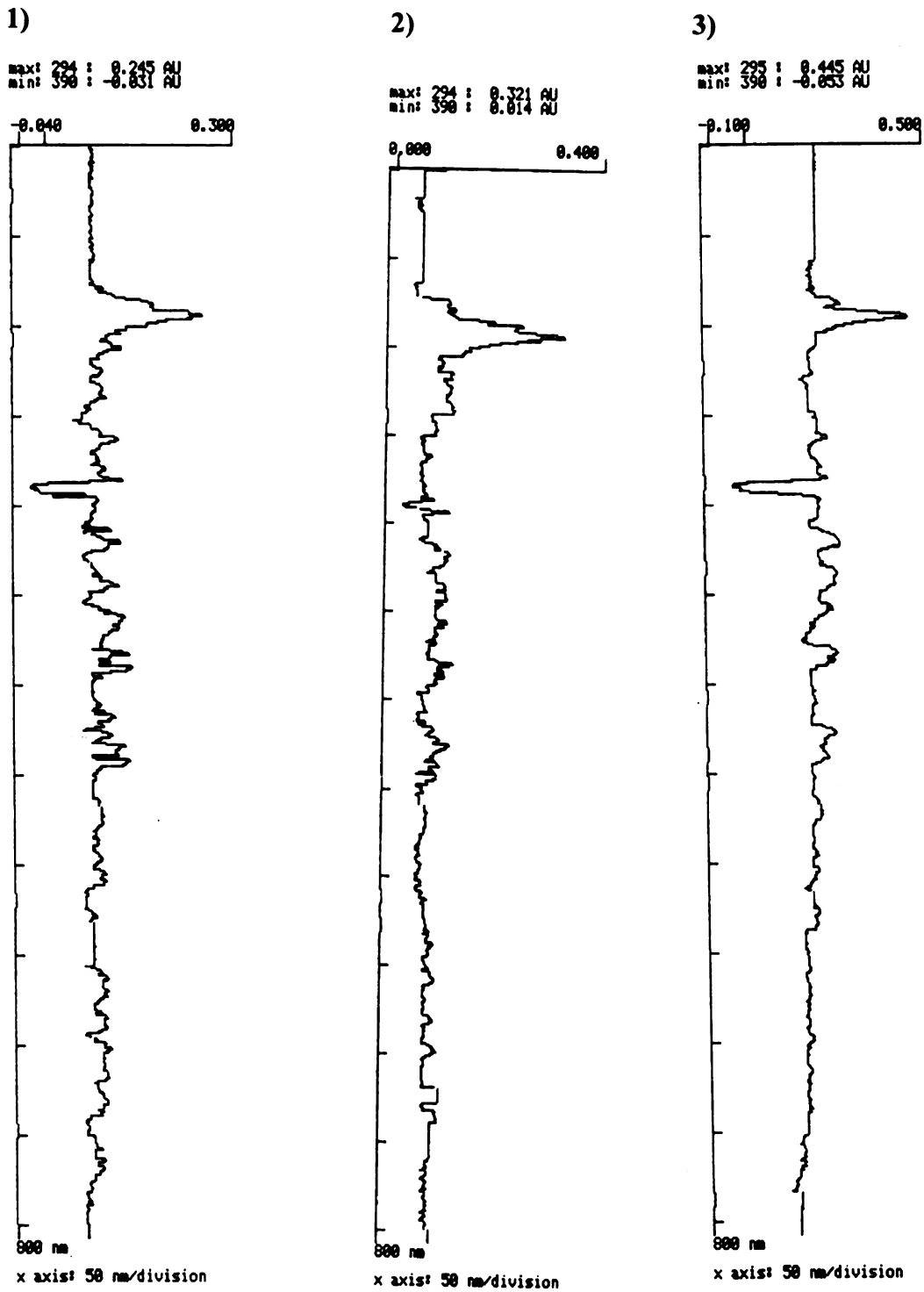

Figure A-5. Light absorbance data for MIP after soaking 25min in an aqueous solution of 5 mM theophylline.

Appendix B: Potentials and Currents Used for Sensitivity and Selectivity Statistical Analysis

Table B-1. Potentials and Currents for B-ITO Evaluated at 1 mM Theophylline.

	Maximum				
	No Thy		**1mM Thy**		
Sensor	*Potential (V)*	*Current (A)*	*Potential (V)*	*Current (A)*	**Current Ratio**
1	-0.635	2.99E-05	-0.635	3.24E-05	1.08
2	-0.290	2.53E-05	-0.290	2.56E-05	1.01
3	0.063	3.57E-04	0.063	3.46E-04	0.97
Average					1.02
	Minimum				
	No Thy		**1mM Thy**		
Sensor	*Potential (V)*	*Current (A)*	*Potential (V)*	*Current (A)*	**Current Ratio**
1	0.349	-7.13E-05	0.349	-8.76E-05	1.23
2	0.600	-9.16E-05	0.600	-9.06E-05	0.99
3	0.428	-5.96E-04	0.428	-5.65E-04	0.95
Average					1.06

Table B-2. Potentials and Currents for MIP-ITO Sensor Evaluated at 1 mM Theophylline.

	Maximum				
	No Thy		**1 mM Thy**		
Sensor	*Potential (V)*	*Current (A)*	*Potential (V)*	*Current (A)*	**Current Ratio**
1	0.094	2.79E-05	0.094	3.01E-05	1.08
2	-0.012	1.46E-04	-0.012	2.05E-04	1.40
3	-0.204	3.26E-04	-0.204	5.78E-04	1.77
Average					1.42
	Minimum				
	No Thy		**1 mM Thy**		
Sensor	*Potential (V)*	*Current (A)*	*Potential (V)*	*Current (A)*	**Current Ratio**
1	0.396	-1.06E-04	0.396	-1.16E-04	1.09
2	0.565	-3.31E-04	0.565	-4.40E-04	1.33
3	0.702	-6.23E-04	0.702	-1.13E-03	1.82
Average					1.41

Table B-3. Potentials and Currents for B-ITO Evaluated at 2 mM Theophylline.

	Maximum				
	No Thy		2 mM Thy		
Sensor	*Potential (V)*	*Current (A)*	*Potential (V)*	*Current (A)*	**Current Ratio**
1	-0.404	2.02E-05	-0.404	2.08E-05	1.03
2	-0.533	4.50E-05	-0.533	5.22E-05	1.16
3	-0.475	1.86E-04	-0.475	1.91E-04	1.03
Average	Minimum				1.07
	No Thy		2 mM Thy		
Sensor	*Potential (V)*	*Current (A)*	*Potential (V)*	*Current (A)*	**Current Ratio**
1	0.875	-7.01E-05	0.875	-8.76E-05	1.25
2	0.879	-1.90E-04	0.879	-1.92E-04	1.01
3	0.788	-2.80E-04	0.788	-2.85E-04	1.02
Average					1.09

Table B-4. Potentials and Currents for MIP-ITO Sensor Evaluated at 2 mM Theophylline.

	Maximum				
	No Thy		2 mM Thy		
Sensor	*Potential (V)*	*Current (A)*	*Potential (V)*	*Current (A)*	**Current Ratio**
1	-0.341	1.01E-04	-0.341	1.21E-04	1.21
2	-0.341	9.65E-05	-0.341	1.14E-04	1.18
3	-0.435	2.51E-05	-0.435	3.22E-05	1.28
Average	Minimum				1.22
	No Thy		2 mM Thy		
Sensor	*Potential (V)*	*Current (A)*	*Potential (V)*	*Current (A)*	**Current Ratio**
1	0.898	-2.84E-04	0.898	-3.21E-04	1.13
2	0.965	-2.65E-04	0.965	-2.95E-04	1.11
3	1.000	-1.15E-04	1.000	-1.55E-04	1.35
Average					1.20

Table B-5. Potentials and Currents for B-ITO Evaluated at 3 mM Theophylline.

	Maximum				
	No Thy		3 mM Thy		
Sensor	*Potential (V)*	*Current (A)*	*Potential (V)*	*Current (A)*	**Current Ratio**
1	-0.063	8.01E-06	-0.063	7.90E-06	0.99
2	-0.655	7.40E-05	-0.655	8.59E-05	1.16
3	0.059	6.85E-06	0.059	8.69E-06	1.27
Average					1.14
	Minimum				
	No Thy		3 mM Thy		
Sensor	*Potential (V)*	*Current (A)*	*Potential (V)*	*Current (A)*	**Current Ratio**
1	0.651	-3.89E-05	0.651	-3.78E-05	0.97
2	1.000	-2.47E-04	1.000	-2.67E-04	1.08
3	0.879	-5.92E-05	0.879	-7.84E-05	1.32
Average					1.12

Table B-6. Potentials and Currents for MIP-ITO Sensor Evaluated at 3 mM Theophylline.

	Maximum				
	No Thy		3 mM Thy		
Sensor	*Potential (V)*	*Current (A)*	*Potential (V)*	*Current (A)*	**Current Ratio**
1	0.071	6.04E-05	0.071	9.21E-05	1.52
2	-0.302	2.62E-05	-0.302	4.20E-05	1.60
3	-0.408	2.57E-05	-0.408	4.75E-05	1.85
Average					1.66
	Minimum				
	No Thy		3 mM Thy		
Sensor	*Potential (V)*	*Current (A)*	*Potential (V)*	*Current (A)*	**Current Ratio**
1	0.592	-1.82E-04	0.592	-2.37E-04	1.30
2	1.000	-1.16E-04	1.000	-1.79E-04	1.54
3	1.000	-1.16E-04	1.000	-1.98E-04	1.70
Average					1.51

Table B-7. Potentials and Currents for B-ITO Evaluated at 4 mM Theophylline.

	Maximum				
	No Thy		4 mM Thy		
Sensor	*Potential (V)*	*Current (A)*	*Potential (V)*	*Current (A)*	**Current Ratio**
1	-0.381	5.57E-05	-0.381	5.58E-05	1.00
2	-0.820	4.53E-05	-0.820	4.77E-05	1.05
3	-0.353	6.00E-05	-0.353	6.10E-05	1.02
Average	**Minimum**				1.02
	No Thy		4 mM Thy		
Sensor	*Potential (V)*	*Current (A)*	*Potential (V)*	*Current (A)*	**Current Ratio**
1	0.788	-1.71E-04	0.788	-1.73E-04	1.01
2	0.879	-1.42E-04	0.879	-1.44E-04	1.02
3	0.408	-1.11E-04	0.408	-8.33E-05	0.75
Average					0.93

Table B-8. Potentials and Currents for MIP-ITO Sensor Evaluated at 4 mM Theophylline.

	Maximum				
	No Thy		4 mM Thy		
Sensor	*Potential (V)*	*Current (A)*	*Potential (V)*	*Current (A)*	**Current Ratio**
1	-0.569	7.60E-07	-0.569	1.00E-06	1.32
2	-0.506	1.87E-05	-0.506	2.12E-05	1.13
3	-0.831	6.85E-05	-0.831	7.60E-05	1.11
Average	**Minimum**				1.19
	No Thy		4 mM Thy		
Sensor	*Potential (V)*	*Current (A)*	*Potential (V)*	*Current (A)*	**Current Ratio**
1	1.000	-1.98E-06	1.000	-3.93E-06	1.98
2	0.910	-8.08E-05	0.910	-8.72E-05	1.08
3	1.000	-2.42E-04	1.000	-2.22E-04	0.92
Average					1.33

Table B-9. Potentials and Currents for B-ITO Evaluated at 1 mM Caffeine.

	Maximum				
	No Thy		1 mM Caf		
Sensor	*Potential (V)*	*Current (A)*	*Potential (V)*	*Current (A)*	**Current Ratio**
1	-0.384	2.25E-05	-0.384	3.31E-05	1.47
2	-0.526	2.13E-05	-0.526	3.65E-05	1.71
3	0.020	6.77E-04	0.020	6.93E-04	1.02
Average	**Minimum**				1.40
	No Thy		1 mM Caf		
Sensor	*Potential (V)*	*Current (A)*	*Potential (V)*	*Current (A)*	**Current Ratio**
1	1.000	-8.82E-05	1.000	-1.22E-04	1.38
2	1.000	-6.89E-05	1.000	-1.45E-04	2.10
3	0.443	-9.72E-04	0.443	-1.04E-03	1.07
Average					1.52

Table B-10. Potentials and Currents for MIP-ITO Sensor Evaluated at 1 mM Caffeine.

	Maximum				
	No Thy		1 mM Caf		
Sensor	*Potential (V)*	*Current (A)*	*Potential (V)*	*Current (A)*	**Current Ratio**
1	-0.400	2.48E-05	-0.400	3.47E-05	1.40
2	-0.028	2.61E-04	-0.028	2.27E-04	0.87
3	-0.028	7.33E-04	-0.028	8.22E-04	1.12
Average	**Minimum**				1.13
	No Thy		1 mM Caf		
Sensor	*Potential (V)*	*Current (A)*	*Potential (V)*	*Current (A)*	**Current Ratio**
1	1.000	-1.06E-04	1.000	-1.21E-04	1.15
2	0.482	-4.61E-04	0.482	-4.21E-04	0.91
3	0.526	-1.20E-03	0.526	-1.38E-03	1.15
Average					1.07

Table B-11. Potentials and Currents for B-ITO Evaluated at 2 mM Caffeine.

	Maximum				
	No Thy		2 mM Caf		
Sensor	*Potential (V)*	*Current (A)*	*Potential (V)*	*Current (A)*	**Current Ratio**
1	-0.486	2.50E-05	-0.486	3.52E-05	1.41
2	-0.581	6.92E-05	-0.581	7.79E-05	1.13
3	-0.286	2.66E-04	-0.286	2.61E-04	0.98
Average	**Minimum**				1.17
	No Thy		2 mM Caf		
Sensor	*Potential (V)*	*Current (A)*	*Potential (V)*	*Current (A)*	**Current Ratio**
1	1.000	-1.09E-04	1.000	-1.42E-04	1.30
2	1.000	-2.45E-04	1.000	-2.92E-04	1.19
3	1.000	-5.68E-04	1.000	-5.27E-04	0.93
Average					1.14

Table B-12. Potentials and Currents for MIP-ITO Sensor Evaluated at 2 mM Caffeine.

	Maximum				
	No Thy		2 mM Caf		
Sensor	*Potential (V)*	*Current (A)*	*Potential (V)*	*Current (A)*	**Current Ratio**
1	-0.373	1.17E-04	-0.373	9.49E-05	0.81
2	-0.302	1.12E-04	-0.302	1.24E-04	1.10
3	-0.467	2.54E-05	-0.467	3.25E-05	1.28
Average	**Minimum**				1.06
	No Thy		2 mM Caf		
Sensor	*Potential (V)*	*Current (A)*	*Potential (V)*	*Current (A)*	**Current Ratio**
1	1.000	-3.11E-04	1.000	-2.93E-04	0.94
2	1.000	-3.23E-04	1.000	-3.25E-04	1.01
3	1.000	-1.14E-04	1.000	-1.30E-04	1.13
Average					1.03

Table B-13. Potentials and Currents for B-ITO Evaluated at 3 mM Caffeine.

	Maximum				
	No Thy		3 mM Caf		
Sensor	*Potential (V)*	*Current (A)*	*Potential (V)*	*Current (A)*	**Current Ratio**
1	-0.067	3.24E-04	-0.067	3.21E-04	0.99
2	-0.377	1.35E-04	-0.377	2.39E-04	1.77
3	-0.051	7.63E-04	-0.051	7.53E-04	0.99
Average					1.25
	Minimum				
	No Thy		3 mM Caf		
Sensor	*Potential (V)*	*Current (A)*	*Potential (V)*	*Current (A)*	**Current Ratio**
1	0.616	-5.46E-04	0.616	-5.66E-04	1.04
2	1.000	-3.12E-04	1.000	-7.86E-04	2.52
3	0.541	-1.22E-03	0.541	-1.24E-03	1.02
Average					1.53

Table B-14. Potentials and Currents for MIP-ITO Sensor Evaluated at 3 mM Caffeine.

	Maximum				
	No Thy		3 mM Caf		
Sensor	*Potential (V)*	*Current (A)*	*Potential (V)*	*Current (A)*	**Current Ratio**
1	-0.392	1.03E-04	-0.392	2.38E-04	2.30
2	-0.455	5.91E-05	-0.455	6.50E-05	1.10
3	-0.102	5.79E-04	-0.102	5.87E-04	1.01
Average					1.47
	Minimum				
	No Thy		3 mM Caf		
Sensor	*Potential (V)*	*Current (A)*	*Potential (V)*	*Current (A)*	**Current Ratio**
1	1.000	-2.74E-04	1.000	-1.07E-03	3.89
2	1.000	-2.17E-04	1.000	-2.46E-04	1.13
3	0.604	-9.80E-04	0.604	-1.02E-03	1.04
Average					2.02

Table B-15. Potentials and Currents for B-ITO Evaluated at 4 mM Caffeine.

	Maximum				
	No Thy		4 mM Caf		
Sensor	*Potential (V)*	*Current (A)*	*Potential (V)*	*Current (A)*	**Current Ratio**
1	-0.361	7.14E-05	-0.361	7.88E-05	1.10
2	-0.600	4.17E-05	-0.600	5.41E-05	1.30
3	-0.506	8.75E-05	-0.506	9.68E-05	1.11
Average					1.17
	Minimum				
	No Thy		4 mM Caf		
Sensor	*Potential (V)*	*Current (A)*	*Potential (V)*	*Current (A)*	**Current Ratio**
1	1.000	-2.67E-04	1.000	-2.64E-04	0.99
2	1.000	-1.59E-04	1.000	-1.39E-04	0.87
3	1.000	-2.14E-04	1.000	-2.25E-04	1.05
Average					0.97

Table B-16. Potentials and Currents for MIP-ITO Sensor Evaluated at 4 mM Caffeine.

	Maximum				
	No Thy		4 mM Caf		
Sensor	*Potential (V)*	*Current (A)*	*Potential (V)*	*Current (A)*	**Current Ratio**
1	-0.357	8.05E-05	-0.357	8.63E-05	1.07
2	-0.530	1.82E-05	-0.530	3.48E-05	1.91
3	-0.341	9.66E-05	-0.341	9.74E-05	1.01
Average					1.33
	Minimum				
	No Thy		4 mM Caf		
Sensor	*Potential (V)*	*Current (A)*	*Potential (V)*	*Current (A)*	**Current Ratio**
1	1.000	-2.88E-04	1.000	-2.53E-04	0.88
2	1.000	-7.68E-05	1.000	-1.05E-04	1.37
3	1.000	-2.56E-04	1.000	-2.11E-04	0.82
Average					1.02

Appendix C: Procedure for Initial Results for Patulin

C.1 Preparation of Patulin MIP

1. Wash and rinse ITO electrodes according to Section 3.3.

2. Silanize ITO electrode in 10% solution (v/v) of 3-MPS in toluene for 6 h at 80°C under nitrogen atmosphere. Rinse electrode with twice with methanol followed by deionized water and dry under nitrogen environment.

3. Combine 0.125 ml MAA, 1.1 ml EDGMA, and 3.3 ml dimethyl sulfoxide (DMSO). Distill by passing solution through a column of inhibitor removal material.

4. Measure 0.5 ml of the above-distilled solution and add 0.01 g of AIBN.

5. Add 200 µl of patulin in DMSO (5 mg patulin in 1ml DMSO)

6. Polymerize in 60°C water bath for 12 h.

7. Break bulk polymer and rinse in 9:1 methanol in acetic acid for 1 hr. Rinse twice with methanol followed by rinsing twice with water.

8. Store sensors in water prior to rebinding and measurement

C.2 Rebinding and Measurement of Patulin MIP

The rebinding and measurement follows the basic procedure of (Blanco-López et al., 2003b) with some modifications:

1. Place sensors in a solution of 1mg patulin in 2ml DMSO for 30 min.

2. Immerse sensors in fresh DMSO for 1 min to remove weakly adhering analyte from surface of sensor.

3. Set up electrochemical cell A with treated sensor at bottom as the working electrode. Place 25 ml of 10% DMSO in deionized water (pH 3) into the electrochemical cell.

4. Perform cyclic voltammetry from –1 V to 1 V at a scan rate of 50 mV/s.